

INJECTION TIMING EFFECTS ON BRAKE FUEL CONVERSION
EFFICIENCY AND ENGINE SYSTEM'S RESPONSES

A Thesis

by

JAMES ELLIOTT MCLEAN, JR.

Submitted to the Office of Graduate Studies of
Texas A&M University
in partial fulfillment of the requirements for the degree of
MASTER OF SCIENCE

August 2011

Major Subject: Mechanical Engineering

Injection Timing Effects on Brake Fuel Conversion Efficiency and Engine System's
Responses

Copyright 2011 James Elliott McLean, Jr.

INJECTION TIMING EFFECTS ON BRAKE FUEL CONVERSION
EFFICIENCY AND ENGINE SYSTEM'S RESPONSES

A Thesis

by

JAMES ELLIOTT MCLEAN, JR.

Submitted to the Office of Graduate Studies of
Texas A&M University
in partial fulfillment of the requirements for the degree of

MASTER OF SCIENCE

Approved by:

Chair of Committee,	Timothy Jacobs
Committee Members,	Jerald Caton
	Adonios Karpetis
Head of Department,	Dennis L. O'Neal

August 2011

Major Subject: Mechanical Engineering

ABSTRACT

Injection Timing Effects on Brake Fuel Conversion Efficiency
and Engine System's Responses. (August 2011)

James Elliot McLean, Jr., B.S., University of Alabama

Chair of Advisory Committee: Dr. Timothy J. Jacobs

Societal concerns on combustion-based fuel consumption are ever-increasing. With respect to internal combustion engines, this translates to a need to increase brake fuel conversion efficiency (BFCE). Diesel engines are a relatively efficient internal combustion engine to consider for numerous applications, but associated actions to mitigate certain exhaust emissions have generally deteriorated engine efficiency. Conventionally, diesel engine emission control has centered on in-cylinder techniques. Although these continue to hold promise, the industry trend is presently favoring the use of after-treatment devices which create new opportunities to improve the diesel engine's brake fuel conversion efficiency.

This study focuses on injection timing effects on the combustion processes, engine efficiency, and the engine system's responses. The engine in the study is a medium duty diesel engine (capable of meeting US EPA Tier III off road emission standards) equipped with common rail direct fuel injection, variable geometry turbo charging, and interfaced with a custom built engine controller. The study found that injection timing greatly affected BFCE by changing the combustion phasing. BFCE

would increase up to a maximum then begin to decrease as phasing became less favorable. Combustion phasing would change from being mostly mixing controlled combustion to premixed combustion as injection timing would advance allowing more time for fuel to mix during the ignition delay. Combustion phasing, in turn, would influence many other engine parameters. As injection timing is advanced, in-cylinder temperatures and pressures amplify, and intake and exhaust manifold pressures deteriorate. Rate of heat release and rate of heat transfer increase when injection timing is advanced. Turbocharger speed falls with the advancing injection timing. Torque, however, rose to a maximum then fell off again even though engine speed and fueling rate were held constant between different injection timings. Interestingly, the coefficient of heat transfer changes from a two peak curve to a smooth one peak curve as the injection timing is advanced further. The major conclusion of the study is that injection advance both positively and negatively influences the diesel engine's response which contributes to the brake fuel conversion efficiency.

DEDICATION

To Mom, Dad, Jackie, and Joe

We have been through a lot but accomplished a lot, too.

ACKNOWLEDGEMENTS

I would first like to thank Dr. Jacobs and for his amazing patience and great guidance while I was at Texas A&M. Secondly, I would like to thank all my colleagues in the Advanced Engines Research Lab, especially Brad, Brandon and Josh for helping me test and compose my data. Without them, this process would have taken much longer. Next, I would like to thank the other two members of my committee, Dr. Caton and Dr. Karpetis. Lastly, I would like to thank my family and friends for supporting me through my two years at Texas A&M.

NOMENCLATURE

BFCE	Brake Fuel Conversion Efficiency
PMEP	Pumping Mean Effective Pressure
IMEP	Indicated Mean Effective Pressure
SOMC	Start of Main Command
SOMI	Start of Main Injection
ROHR	Rate of Heat Release
ROHT	Rate of Heat Transfer
MFB	Mass Fraction Burned
VGT	Variable Geometry Turbocharger
EGR	Exhaust Gas Recirculation
LHV	Lower Heating Value
HHV	Higher Heating Value
ID	Ignition Delay
TDC	Top Dead Center
FMEP	Friction Mean Effective Pressure

TABLE OF CONTENTS

	Page
ABSTRACT	iii
DEDICATION	v
ACKNOWLEDGEMENTS	vi
NOMENCLATURE	vii
TABLE OF CONTENTS	viii
LIST OF FIGURES	x
LIST OF TABLES	xiii
1. INTRODUCTION.....	1
1.1 Motivation	1
1.2 Background	3
1.3 Objective	8
2. EXPERIMENTAL METHODOLOGY	9
2.1 Engine.....	9
2.2 Measurements.....	13
2.2.1 Non In-cylinder Pressure and Temperature Measurements	13
2.2.2 Fuel Flow Measurements	14
2.3.3 Dynamometer	15
2.3 Fuel Used in the Test.....	16
2.4 Data Collection.....	16
2.4.1 Rate of Heat Release Calculation.....	20
2.5 Uncertainty Calculations	25
3. RESULTS.....	26
3.1 Effects of Injection Timing on Premixing.....	26
3.2 Effects of Injection Timing on Combustion Efficiency	33
3.3 Effects of Injection Timing on In-cylinder Temperatures and Pressures.....	34

	Page
3.4 Effects of Injection Timing on Rate of Heat Transfer	37
3.5 Effects of Injection Timing on Rate of Heat Transfer due to Surface Area	42
3.6 Effects of Injection Timing on Mean Effective Pressures	48
3.7 Effects of Injection Timing on Intake and Exhaust Manifold Pressures and Turbocharger Speed.....	49
3.8 Effects on Location of Peak Pressure.....	54
4. CONCLUSIONS AND SUMMARY	57
REFERENCES	59
VITA	61

LIST OF FIGURES

FIGURE		Page
1	Phases of Diesel Combustion.....	5
2	VGT Example from Volvo.....	11
3	Fuel System Diagram.....	12
4	Solenoid Injector.....	13
5	Fuel Energy Flow vs. Start of Main Command.....	18
6	Control Volume Illustration.....	22
7	Torque and BFCE as Functions of Start of Main Command (in Degrees After Top Dead Center, or ⁰ ATDC) for (a) 1400 RPM/50 lb-ft, (b) 1400 RPM/250 lb-ft, (c), 2400 RPM/50 lb-ft and (d) 2400 RPM/150 lb-ft.....	27
8	Ignition Delay, Start of Main Injection and Start of Main Combustion vs Start of Main Command for (a) 1400 RPM 50 lb-ft and (b) 250 lb-ft.....	28
9	Ignition Delay, Start of Main Injection and Start of Main Combustion vs Start of Main Command for 2400 RPM (a)50 lb-ft and (b)150 lb-ft.....	29
10	Rate of Heat Release and Mass Fraction Burned vs Crank Angle for 1400 RPM 50 lb-ft with Injection Timings of -4°, -10°, and -22° ATDC.....	30
11	Rate of Heat Release and Mass Fraction Burned vs Crank Angle for 1400 RPM 250 lb-ft with Injection Timings of -4°, -13°, and -22° ATDC.....	31
12	Rate of Heat Release and Mass Fraction Burned vs Crank Angle for 2400 RPM 50 lb-ft with Injection Timings of -10°, 17.5°, and -25° ATDC.....	32
13	Rate of Heat Release and Mass Fraction Burned vs Crank Angle for 2400 RPM 150 lb-ft with Injection Timings of -10°, -22.5°, and -25° ATDC...	33
14	Combustion Efficiency vs Start of Main Command for All Speeds and Loads.....	34

FIGURE	Page
15 Pressure and Temperature Maximums vs Start of Main Command for the 1400 RPM Cases	36
16 Rate Pressure and Temperature Maximums vs Start of Main Command for the 2400 RPM Cases.....	36
17 Rate of Heat Transfer vs Crank Angle for the 1400 RPM and 50 lb-ft Case	37
18 Rate of Heat Transfer vs Crank Angle for the 1400 RPM 250 lb-ft Case	38
19 Rate of Heat Transfer vs Crank Angle for the 2400 RPM 50 lb-ft Case ...	39
20 Rate of Heat Release vs Crank Angle for the 2400 RPM 150 lb-ft Case...	39
21 Heat Release Coefficient vs Crank Angle in the Low Speed Low Load Case	41
22 Bulk Heat Release Coefficient vs Crank Angle in the High Speed High Load Case	42
23 Bulk Gas Temperature (K) and Surface Area (m ²) vs Crank Angle (°) for the -4°, -10°, and -22° ATDC Timings of the Low Speed Low Load Test Conditions.	44
24 Bulk Gas Temperature (K) and Surface Area (m ²) vs Crank Angle (°) for the -4°, -13°, -22° ATDC Injection Timings for the Low Speed High Load Case	45
25 Bulk Gas Temperature (K) and Surface Area (m ²) vs Crank Angle (°) for the -10°, -17.5°, -25° ATDC Injection Timings for the High Speed Low Load Case	46
26 Bulk Gas Temperature (K) and Surface Area (m ²) vs Crank Angle (°) for the -10°, -22.5°, -25° ATDC Injection Timings for the High Speed High Load Case	47
27 Net Indicated Mean Effective Pressure, Brake Mean Effective Pressure, and Friction Mean Effective Pressure vs Start of Main Command for Low Speed and Low Load Case	48

FIGURE	Page
28 Net Indicated Mean Effective Pressure, Brake Mean Effective Pressure, and Friction Mean Effective Pressure vs Start of Main Command for the High Speed High Load Case	49
29 Intake and Exhaust Manifold Pressures and Turbo Speed vs. Start of Main Command for Low Speed Low Load Test Condition	50
30 Exhaust Manifold Temperature vs. Start of Main Command for All Test Conditions	51
31 Intake and Exhaust Manifold Pressures and Turbo Speed vs. Start of Main Command for Low Speed High Load Test Condition	51
32 Intake and Exhaust Manifold Pressures and Turbo Speed vs. Start of Main Command for High Speed Low Load Test Condition	52
33 Intake and Exhaust Manifold Pressures and Turbo Speed vs. Start of Main Command for High Speed High Load Test Condition.....	53
34 Location of Peak Pressure verses Start of Main Command for All Test Conditions	55
35 Location of Peak Pressure verses Brake Fuel Conversion Efficiency for Low Load Cases	56
36 Location of Peak Pressure verses Brake Fuel Conversion Efficiency for High Load Cases	56

LIST OF TABLES

TABLE		Page
1	Engine Specifications.....	10
2	Fuel Properties.....	16
3	Engine Test Matrix.....	17
4	Measured and Calculated Values	19

1. INTRODUCTION

1.1 Motivation

Diesel engines have been in use for over 100 years and have penetrated daily life. Perhaps it is safe to say that all commercial products are harvested or transported by at least one machine powered by a diesel engine. Everything from an ocean going cargo ship to an asphalt laying machine is powered by diesel. Diesel engines offer many advantages to gasoline fueled spark ignition (SI engines) engines. The diesel engine is practically perceived to be more durable than the gasoline engine, because diesel components are built to last longer and do not require an external ignition system. Diesel engines deliver higher efficiencies than their gasoline powered counterparts at the same power rating because of their higher compression ratio and ability to operate with lean equivalence ratios. This has made it the focus of many automakers as they try to improve vehicle fleet fuel economy. With the lawmakers mandating that the Corporate Average Fuel Economy (CAFE) move to 30 mpg for trucks and 39 mpg for passenger cars by 2016, for an average of 35.5 mpg, overall efficiency of engines must be examined to find out how it can be improved. However, there are some drawbacks to the diesel engine.

This thesis follows the style of *Journal of Engineering for Gas Turbines and Power*.

They typically produce more nitric oxide and particulate matter emissions than conventional gasoline fueled engines. The increase in nitric oxide is from the elevated in-cylinder temperatures and pressures in a diesel engine compared to the in-cylinder conditions in a gasoline engine. Nitric oxide formation is mainly thermally driven so the increased temperatures will cause higher levels of NO_x . The particulate matter emissions arise from the local temperatures in the cylinder becoming too low to have good combustion of the fuel. This happens when engines are tuned to produce lower nitric oxide levels. There is a well-documented trade-off between the NO_x and PM emissions in conventional diesel combustion. This makes it more difficult to meet the strict emission standards, because traditional after treatment devices do not work with diesel engines. Traditional catalytic converters that are used with gasoline engines require that the equivalence ratio be near stoichiometric and because diesel engines usually run lean they cannot be used. Engine designers, however, have implemented technologies to help counteract the emission problems like: high pressure common rail fuel systems, exhaust gas recirculation, variable geometry turbo chargers, and exhaust after treatment technologies like Selective Catalytic Reduction (SCR) and particulate matter filters.

There is a tradeoff between emissions and efficiencies that has to be taken into consideration. As the after treatment technologies get better a focus on efficiency can be allowed. A good judge of an engine's overall efficiency is the brake fuel conversion efficiency (BFCE), because it assesses the effectiveness of the engine to deliver power at the expense of the fuel. The BFCE is a function of power and fuel flow into the engine.

1.2 Background

Fuel injection timing effects on engine behavior, including efficiency, power, and emissions, are very well-documented (eg.[1-4]). A widely known action that has a direct effect on engine efficiency is the injection timing of fuel inside the engine cylinder.

Usually an advance in injection timing favors engine efficiency up to a point beyond which efficiency is then reduced [4]. Modern-day fuel systems, which offer control over injection timing, number of injections, injection duration and injection pressure, allow the engineer to explore numerous fuel and injection strategies [5, 6]. Brake fuel conversion efficiency is affected by many things including but not limited to: friction mean effective pressure (FMEP), ratio of specific heats, heat transfer, combustion phasing, and combustion efficiency. Effective pressures are a good way of examining engine performance as well, because they are independent of both engine size and speed. If torque is used for engine comparison, a larger engine will always look better. If power is used as the comparison, speed becomes very important. All mean effective pressures (mep) are defined by work divided by displaced volume as seen in Equation 1. For brake mean effective pressure (BMEP), the work is the brake work as measured by the dynamometer and for indicated mean effective pressure (IMEP) the work term is the indicated work that comes from the in-cylinder pressure reading. The FMEP is the work lost to friction, driving accessories like fuel pumps and alternators, and other losses over the displaced volume and can be found by subtracting BMEP from the IMEP as seen in Equation 2.

$$mep = \frac{w}{\Delta v} \quad (1)$$

$$fmep = imep - bmep \quad (2)$$

Since the values of the total FMEP indicate the net power loss due to the pumping loss of gas exchange, the mechanical friction losses of gas exchange, the mechanical friction losses of piston, bearing, transmission and valve train systems, and the driving power of auxiliaries, it is difficult to estimate each of the power losses delivered to these categories in detail [7]. FMEP changes BFCE because it will detract from the torque delivered to the dynamometer. So if everything else is held constant, BFCE will increase and decrease with FMEP. The ratio of specific heats (γ) is the specific heat capacity at constant pressure (C_p) over the specific heat capacity at constant volume (C_v) which can be seen in Equation 3.

$$\gamma = \frac{C_p}{C_v} \quad (3)$$

The ratio of specific heats is important to BFCE because it affects the fuel conversion efficiency. As the equivalence ratio is decreased below unity, the efficiency increases. This occurs because the burned gas temperatures after combustion decrease, decreasing the burned gas specific heats and thereby increasing the effective value of γ over the expansion stroke. The efficiency increases because, for a given volume-expansion ratio, the burned gases expand through a larger temperature ratio prior to exhaust; therefore, per unit mass of fuel, the expansion stroke work is increased. Heat transfer changes BFCE because the more heat that is lost through heat transfer the less energy that is available to do useful work. Combustion efficiency is important because it describes how much of the delivered fuel is combusting and releasing energy to be available to do work useful or otherwise. In studies of engines, there are two ways work can be described indicated or brake. Indicated work is the work that is calculated using the in-

cylinder pressure measurement. Gross indicated work is the work delivered to the piston over the compression and expansion strokes only while net indicated work is the work delivered to the piston over the entire four-stroke cycle. Brake work on the other hand is the usable power delivered by the engine to the load. Basically, indicated work is the maximum available work in the engine and the brake work is the actual work available to be used.

As stated earlier, combustion phasing affects BFCE as well as other engine efficiencies. Diesel combustion is divided into four general phases: ignition delay, pre-mixed (rapid) combustion, mixing controlled combustion, and late combustion [8].

Figure 1 shows the stages of combustion on a rate of heat release to crank angle graph.

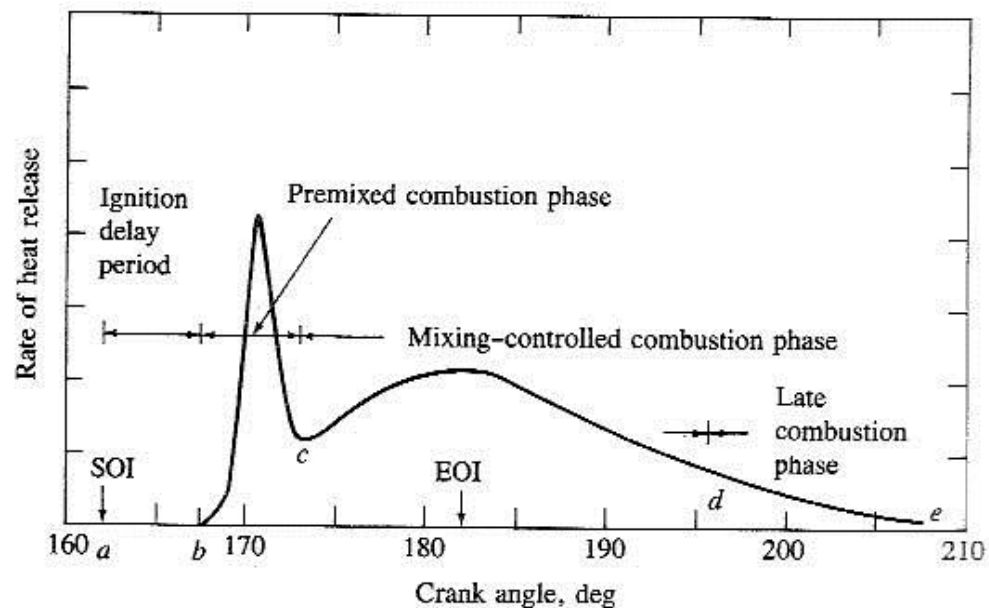


Figure 1: Phases of Diesel Combustion[8].

In the figure, SOI is start of injection and EOI is end of injection. The ignition delay period is from $a-b$. The premixed combustion phase which is characterized by the steep slope of the rate of heat release curve lasts from $b-c$. The mixing-controlled combustion phase, which has a maximum in the rate of heat release curve but the slopes leading to and from the maximum are not as steep as the premixed combustion phase, is from $c-d$. The late combustion phase that ends combustion is from $d-e$.

Ignition delay, in the context of engine combustion, is defined as the crank angle separation between start of injection and start of combustion. In this period, the fuel is injected at a high speed into the cylinder and starts the atomization process. The physical processes of the fuel heating up, vaporizing, and mixing with the cylinder air control the duration of the ignition delay. Advancing fuel injection increases the delay period as well as the maximum rate of heat release. The total burning time is appreciably reduced with injection advance because the percentage of the fuel that is atomized in the delay is higher. If, however, the total time from the beginning of injection to the end of combustion is considered, the reduction to this total time with injection advance is much less[9]. At the end of the ignition delay, when air-fuel ratios and temperatures are favorable for auto-ignition, rapid, or premixed, combustion begins.

The premixed combustion causes the temperature and pressure inside the cylinder to rise and cause a transition to mixing-controlled combustion. The advance in injection timing results in a considerable increase of the peak pressure in the cylinder [4]. The higher pressures are due to the quick burn rate of the fuel during the premixed phase. It is observed that all measures leading to an increase of engine efficiency result

in an increase of the engine maximum combustion pressure [10]. The burning rate of fuel is important in all reciprocating engines because it directly controls the cycle efficiency, the noise emitted from the engines and the peak pressure to which the engine components are subjected[11].

During mixing-controlled combustion, fuel can be (and typically is) injected into the reaction zone within the cylinder. This causes the rate of heat release to partially depend on the rate of fuel injection and its consequent physical evolution from liquid to vapor. The rate of heat release during the mixing controlled combustion period typically requires more time, depending on the quantity of fuel being injected (as determined by the desired torque of the engine). The last phase of combustion is late combustion. Late combustion results from the unburned hydrocarbons present in the exhaust gases; such burning provides little additional heat release to the total heat release.

Changes in injection timing change the position of the piston, and thus cylinder pressure and temperature, at injection. Consequently, some important influencing parameters such as ignition delay, are changed [12]. The change in ignition delay causes changes throughout the remaining processes. Typically, a longer ignition delay will allow more fuel to become premixed, thus increasing the extent of premixed combustion (and reducing the amount of mixing-controlled combustion). The relative fractions of premixed and mixing-controlled combustion can have positive or negative consequences on engine efficiency, power, and emissions. Increasing the injection advance increases the delay period and with it the maximum rate of heat release[1].

1.3 Objective

The objective of this study is to fill in gaps in available literature on how diesel engines respond to changes in injection timing. In the research done for this study, there was a lot of literature available on how injection timing affected the phases of combustion, but information on how changes in phasing and injection timing would affect other engine response is lacking. There will be a focus on BFCE and what factors affect BFCE specifically, because of its ability to represent an engine's overall efficiency well. However, injection timing effects on other parameters, such as: exhaust manifold temperature and pressure, rate of heat release, rate of heat transfer, PMEP, FMEP, turbocharger speed, IMEP, and the phases of combustion, will also be discussed in detail.

2. EXPERIMENTAL METHODOLOGY

2.1 Engine

The study uses data collected from a production four-cylinder medium-duty diesel engine. It is a Power Tech Plus Series diesel, model 4045HF485 produced by John Deere. The engine specifications are summarized in Table 1. The engine is outfitted with a variable geometry turbocharger (VGT), exhaust gas recirculation (EGR), and a custom built engine controller (Drivven Inc., San Antonio, Texas). The engine controller allows for control of many parameters of the engine but for this study those that matter most are the controller's ability to control injection timing, injection duration, and rail pressure. The engine came stock to meet Tier III emission standards. To accomplish this, the engine comes with a variable geometry turbocharger. The variable geometry refers to the ability of the vanes inside the turbocharger to change position to allow for more or less air to be compressed. As the vanes change position, the intake manifold will change pressure. Figure 2 shows an example of a VGT (in the picture it is called a VNT but they are the same concept) and describes how the vanes are actuated to accommodate different operating conditions [13]. On the stock John Deere Engine, the vane position is controlled by an arm connected to a small electric motor. In the study, however, the position of the vanes was held constant by fixing the control arm to a plate. During the tests, the speed of the turbo was limited to 95000 rpm so to not subjugate the turbocharger to excessive speeds and intake manifold to unnecessary pressures.

Table 1: Engine Specifications

Number of Cylinders	4
Compression Ratio	17.0:1
Bore (in, mm)	4.19, 106
Stroke (in,mm)	5, 127
Displacement (in ³ , L)	275, 4.5
Valves per Cylinder Int-Ext	2-2
Aspiration	VGT
Charge Air Cooling System	Air-to-Air
Peak Power (hp, kW @2400 rpm)	154, 115
Peak Torque (ft-lb, N-m @1400 rpm)	424, 575
Rated Speed (rpm)	2400
Breakaway Speed (rpm)	2470

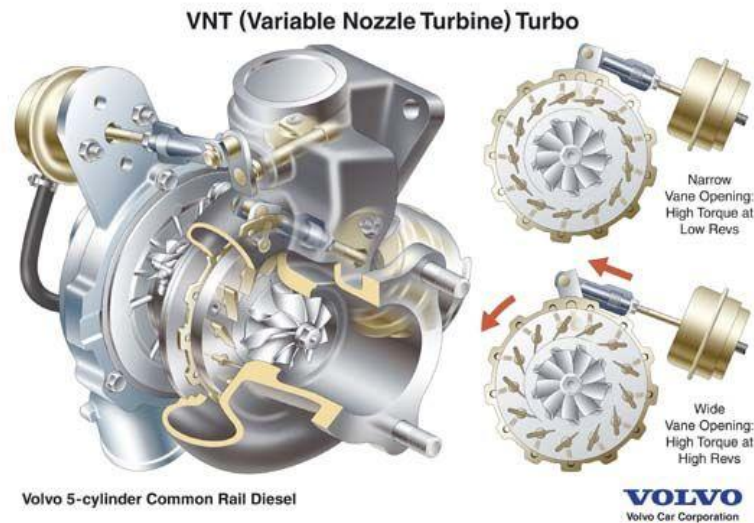


Figure 2: VGT Example from Volvo [13].

The next technology that the engine is equipped with so that it can comply with Tier III standards is exhaust gas recirculation (EGR). EGR is the practice of inducting exhaust gases along with fresh air during the intake stroke this can be accomplished by opening the exhaust valve during the intake stroke or by introducing an EGR valve between the intake and exhaust manifolds. The John Deere engine used in this study was outfitted with and EGR valve. Another stock technology to comply with tier III emissions standards was the common rail fuel injection system. The system, which can be seen in Figure 3, is made up of a rail that feeds all 4 injectors. The rail is fed by a high pressure pump that can be pressurized up to 1800 bar but is never run at pressures that high. The fuel leaves the rail at high pressure and enters the injectors; whatever is not used is returned through the fuel leak-off line. The injectors themselves are standard solenoid injectors controlled by the engine's ECU. Figure 4 is a detailed drawing of the

injectors used in the engine [14]. The injector's nozzles have 6 holes with a diameter of .18mm to provide a well-developed fuel spray.

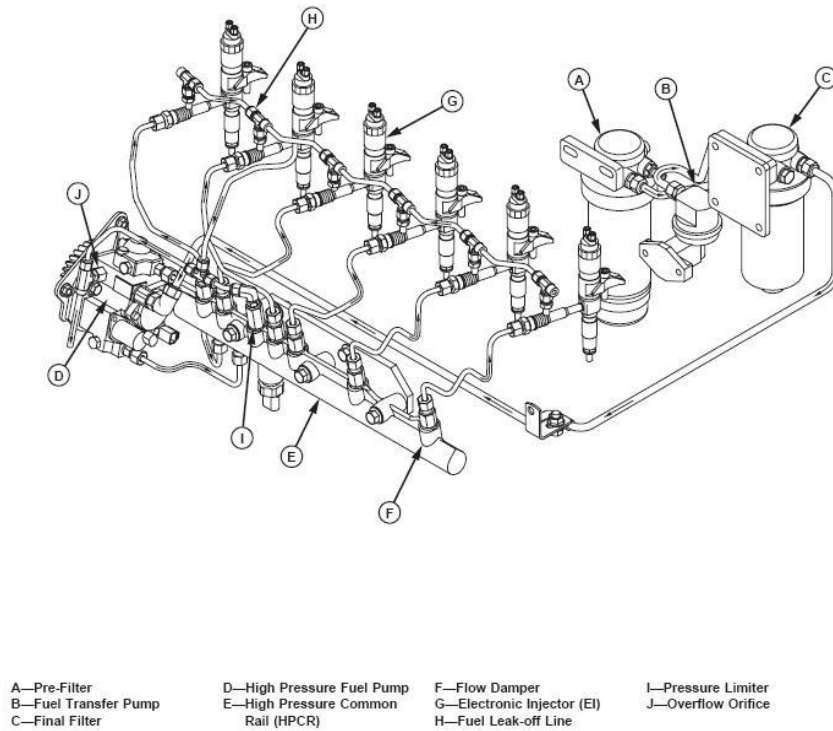


Figure 3: Fuel System Diagram [14].

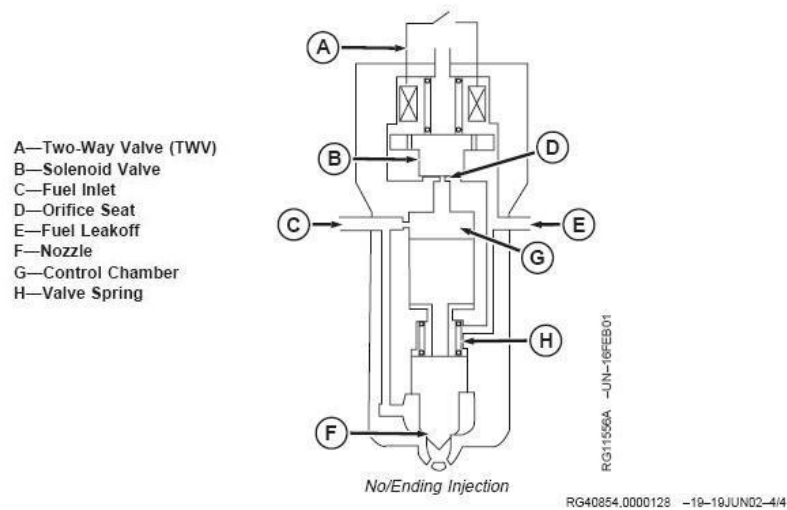


Figure 4: Solenoid Injector[14].

2.2 Measurements

2.2.1 Non In-Cylinder Pressure and Temperature Measurements

All the pressure readings done in the intake and exhaust systems are done by four transducers from Omega Engineering (Stamford, Connecticut). The PX309-050A5V transducer models have a pressure range from 0 to 3.45 bar with an error of 0.25%. There are two types of thermocouples used to measure the temperatures; they are all type K thermal couples though. The type K thermocouples use nickel and chromium or aluminum for the wire set. The two metals cause an electric voltage that can be correlated into a temperature. Three thermocouples come from Temprel Incorporated (Boyer, Michigan) which are model number T-26. These three thermocouples are used to measure the exhaust manifold, post turbocharger exhaust, and pre compressor intake temperatures. The T-26 thermocouple can measure temperatures up to 1650°F (900°C), with an error of 1.1°C. The other thermocouple used to measure the intake manifold

temperature is from Omega Engineering (Stamford, Connecticut). It has a one-eighth of an inch diameter, can measure temperatures up to 500°F (260°C), and has an error of 2.2°C. Temperature and barometric pressure are measured at the air intake using temperature and pressure sensors from Omega Engineering.

2.2.2 Fuel Flow Measurements

The fuel flow into the engine is measured using a piston type flow meter. The flow meter works in conjunction with a vapor eliminator and fuel level control to supply the engine with as constant and measurable flow of fuel possible. All components were made by Max Machinery (Healdsburg, CA). The fuel is first pumped from 55 gallon drums of fuel in a fire cabinet to a SHURflo Bronze Close-Coupled Self-Priming Flexible Impeller Pump model number MRB9001. From the pump, the fuel then passes through a three-way valve. From the three-way valve, the fuel can go to the vapor eliminator or go through a valve and back into the fuel barrel. The valve lets us regulate the pressure of the vapor eliminator and meter. The vapor eliminator removes air and fuel vapor bubbles in the fuel supply line before the fuel gets to the fuel meter. It operates at a maximum pressure of 5.17 bar and depending on the fuel flow rate it can eliminate air at a rate of 300 to 2100 cubic centimeters (cc) per minute. The flow meter is after the vapor eliminator. The flow meter has four radial pistons which rotate around a central shaft. The fuel is measured using the displacement of each piston to determine the mass flowing. An electric meter is connected to the crankshaft and turns the fuel measurement into a voltage between 0 and 10 Volts that is sent to the data acquisition system. After the flow meter, the fuel enters the level controller. There are two main

functions of the level controller: 1) to supply fuel to the engine and 2) accept the bypass fuel from the common rail injection system. It accomplishes this by having a supply tank. The supply tank level is controlled by a mechanical float indicator. The tank is equipped with a vent system that keeps vapor or bubbles out of the fuel line. It has a flow rate of 1500 cc per minute for diesel with a maximum inlet pressure of 1.38 bar. The tank inside of the level controller has a maximum volume of 202 cc at 0.69 bar. All of the metering equipment can operate at a max temperature of 93.3 °C. The fuel system measurements are important because of how BFCE is calculated in this study. BFCE is a function of brake power (P_b) (kW), fuel flow rate (\dot{m}) (g/s), and lower heating value (LHV) (MJ/kg). The equation can be seen in Equation 4. Because of BFCE's dependence on fuel flow rate and brake power, the fuel rate measurement and the brake power measurements are very important.

$$BFCE = \frac{P_b}{\dot{m} * LHV} \quad (4)$$

2.2.3 Dynamometer

The engine is loaded using a direct current dynamometer produced by General Electric. It is capable of 110 kW of power absorption and uses a Wheatstone bridge strain gauge that measures the force used to calculate the torque produced by the engine. The energy absorbed by the dynamometer is fed back into the electrical grid. Loading on the engine is done by introducing an electric current into the dynamometer. This current gives the dynamometer resistance to spin. The engine compensates by adding more fuel to increase the power. An increase in power helps the engine to overcome the resistance from the dynamometer and maintain a set speed on the engine controller. The control

can be set to a specified torque and speed. During this test speed was controlled and torque was varied by adjusting the fuel injection duration (i.e., fuel quantity).

2.3 Fuel Used in the Test

The fuel used for the test was Diesel #2 purchased from Producers Cooperative Association (Bryan, TX). It is intended for off highway use by agricultural equipment. A portion of the fuel was measured by Southwest Research Institute (San Antonio, Texas) and the rest of the fuel was assumed to have the same qualities. The fuel was measured to have a lower heating value (LHV) of 43.008 MJ/kg and stoichiometric air/fuel ratio of 14.44 a complete list of properties is available in Table 2.

Table 2: Fuel Properties

HHV (MJ/kg)	45.843
LHV (MJ/kg)	43.008
H/C Ratio	1.862313
Stoicheometric A/F Ratio	14.44

2.4 Data Collection

Data was collected for two test speeds, two test loads, and seven injection timings at each speed and load condition. Table 3 shows the complete test matrix. The two speeds were 1400 rpm and 2400 rpm (low and high speeds). For the low speed tests,

the two loads that are investigated are 50 and 250 lb-ft (67.8 and 339 N-m). For the high speed, the loads researched are 50 and 150 lb-ft (67.8 and 203 N-m). At the high speeds, 250 lb-ft of torque caused some problems with turbocharger speed and interference in the control speeds so 150 lb-ft was investigated instead. For each speed and load combination seven injection timings are investigated to allow for a large enough range to catch the peak efficiencies.

Table 3: Engine Test Matrix

Speed (RPM)	Load (lb-ft)	Injection Timing (°BTDC)	EGR Valve Position	Speed (RPM)	Load (lb-ft)	Injection Timing (°BTDC)	EGR Valve Position
1400	50	4°-22° BTDC in 3° increments	Completely Closed (0% EGR)	2400	50	10°-25° BTDC in 2.5° increments	Completely Closed (0% EGR)
	250				150		

For the low speed tests, the rail pressure was held at 900 bar at the high speed the rail pressure was set to 1250 bar. For all tests the fuel flow rate was kept as constant as possible. To accomplish this injection duration was varied slightly. The maximum deviation was for the 1400 250 test point but it only accounted for 5% of the minimum

flow rate taken. Figure 5 shows the fuel energy flow as a function of start of main command for all speeds and loads. As can be seen the flows are relatively consistent.

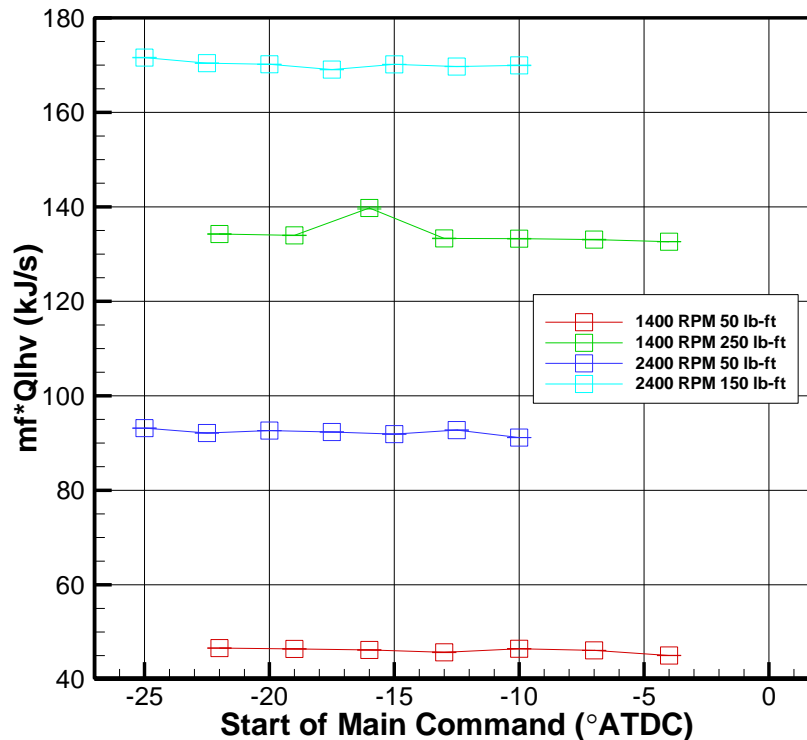


Figure 5: Fuel Energy Flow vs. Start of Main Command.

The turbocharger's vane position was held constant throughout the test as to not have the vane position affect the outcome of the tests. To set the position the engine was allowed to come to a steady state at 2400 RPM and 100 lb-ft. This condition was chosen because it would insure that the turbocharger would not exceed the recommended maximum speed. Once there the turbocharger's vane position was varied until a maximum torque

was accomplished. That position was then locked down and marked so that it could be repeated without much effort. The measurements and calculations are used to generate the data that support the analysis of this study. Table 4 gives a summary of what is measured and calculated and how the measurement or calculation was done. Start of injection is when the fuel first begins to enter the cylinder through the injector nozzle and is measured using a needle lift sensor that has been imbedded in the injector. While the start of ignition is when the combustion starts and is defined in this study as 1% mass fraction burned.

Table 4: Measured and Calculated Values

Parameter	How determined	Notes
Injector needle lift signal	Measured	Needle motion (hall effect sensor)
In-cylinder pressure	Measured	Pegged using methods in [15]
Indicated Mean Effective Pressure	Calculated	In-cylinder pressure and volume
Net rate of heat release	Calculated[16-19]	In-cylinder pressure and volume, F/A, fuel flow rate, EGR Level
Mass Fraction burned	Calculated	Same as net rate of heat release
Engine ignition delay	Calculated	Injector needle lift signal and 1% burn location [8]
Combustion duration	Calculated	1% and 90% burn locations
Start of Injection In-cylinder Pressure	Measured	Based on needle motion, in-cylinder conditions are approximated based on pressure
Brake Fuel Conversion Efficiency	Calculated	Power divided by fuel energy delivered

2.4.1 Rate of Heat Release Calculation

In-cylinder pressure is used in the calculation of rate of heat release. A digital filter is employed to remove high frequency noise from the raw pressure measurements to provide relatively smooth rate of heat release profiles. The filter is a low pass zero phase Infinity Impulse Response (IIR) filter. A filter order of three is used with a cutoff frequency of approximately 10% of the sampling frequency. After the averaging of 300 cycles, the filtering is done. The filter properties were established so that the pressure derivative maximums related with combustion events were minimally influenced both in peak value and width. Under the assumption of a single zone mixture and ideal gas behavior, the rate of apparent heat release is calculated using the First Law of Thermodynamics. In the single zone model, the control volume is defined to be concurrent with the cylinder volume and to be initially composed of air and exhaust residual. The mass flow rate results in the experimental pressure trace if the fuel instantaneously reacted to equilibrium products upon entering the combustion chamber. Multiplying this apparent mass flow rate by the heating value of the fuel results in the apparent heat release. The real power of the heat release analysis in a single zone model is that it offers a sensitive measure for comparing the pressure traces as engine operating conditions are changed [20]. The energy balance, which tracks all energy transfers and storage in the cylinder, is shown below in Figure 6. Equation 5 based on the first law of thermodynamics, defines sign conventions and shows how each term can influence the heat release rate.

$$\delta Q_{HT} - \delta W + dU_{cv} = \delta Q_{HR} \quad (5)$$

δQ_{HR} is the apparent heat release rate, δW is the work rate of the piston, dU_{CV} is the rate of internal energy change, and δQ_{HT} is the heat transfer. The work term accounts for the work done by or on the piston as the cylinder contents are compressed or expanded. A positive work term decreases the calculated heat release rate. The internal energy term accounts for the change in energy storage of the cylinder contents as the temperature changes. An increase in internal energy is used in the calculation of rate of heat release. Finally, due to the combustion event there is an increase in cylinder energy, termed heat release that is modeled simply as another heat transfer source. However, the energy release is due to chemistry mechanisms in the cylinder but, including the detailed chemical kinetic mechanisms would add unnecessary complication to the calculation which is intended to be simple. The simplification of modeling the combustion as a simple heat transfer source is the reason the calculation is termed apparent heat release.

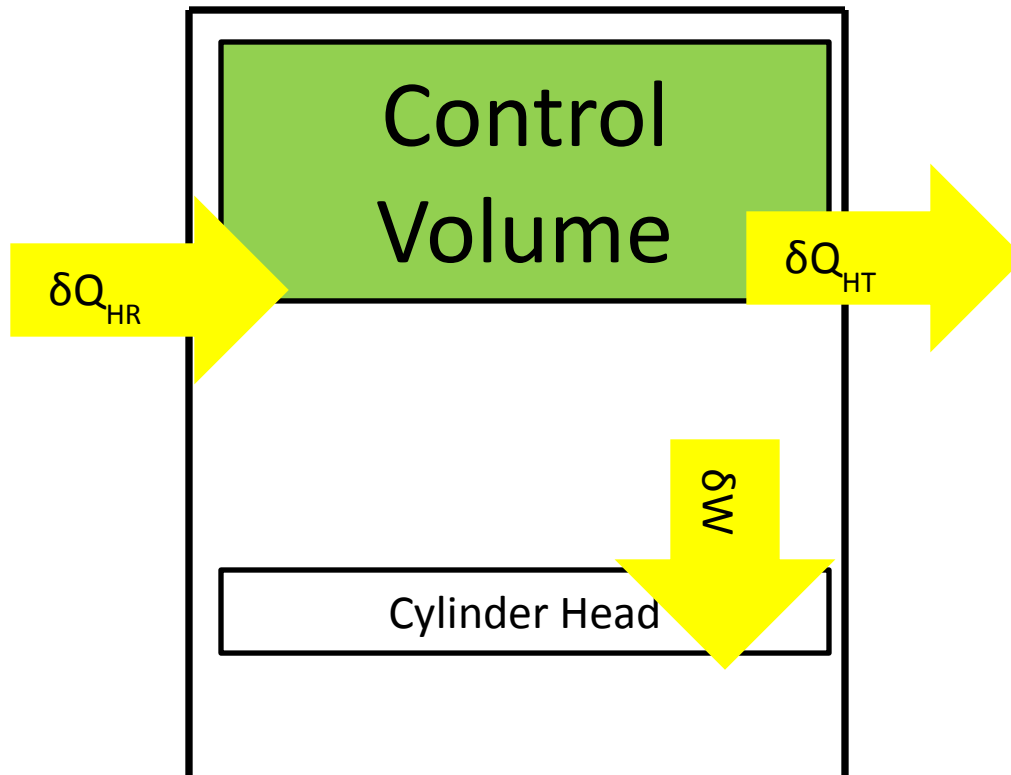


Figure 6: Control Volume Illustration.

δW , dU_{CV} , and δQ_{HT} need to be calculated so that δQ_{HR} can be found. The work term is calculated from the cylinder geometry and pressure measurement as follows, where p is pressure and dV is the rate of volume change of the cylinder.

$$\delta W = p * dV \quad (6)$$

The internal energy term assumes that the mixture behaves as an ideal gas. Because of the ideal gas behavior, the internal energy is only a function of temperature, and the mixture components individual properties are additive.

$$dU_{cv} = \sum_i x_i * m * C_{v,i} * dT \quad (7)$$

The term x_i , represents the mass fraction, m is total trapped mass heat, $C_{v,i}$ is the specific heat of the individual species, and dT is the temperature rate of change. The ideal gas assumption permits the use of $C_v dT$ term to calculate the internal energy change of each species and the use of the summation over each species. The species mass fractions, specific heat, and the temperature change all must be determined individually. The ideal gas law also sanctions a simple application to calculate the temperature. The pressure measurement is combined with the cylinder geometry, known trapped mass, and the mixture gas constant at a given increment to solve the ideal gas law equation for the temperature. Both the species concentrations and the specific heat values are calculated based on information in the JANAF tables [21]. These computerized tables have detailed equation fits for experimentally determined species properties. Also included in the tables, are species equilibrium mechanism constants that aid in determining the equilibrium concentrations for a specific reaction. These equations allow for the simultaneous solution of a number of important species equilibrium mechanisms that are included in the calculation. Like the water gas shift equation which is important because it is used to determine the concentrations of H_2O , CO_2 , H_2 , and CO . Subsequently, knowing the species concentrations that correspond to a given temperature and pressure along with the species specific heats allow for the calculation of the mixture internal energy.

The last term, heat transfer, is calculated using a simple heat transfer model.

$$\delta Q_{HT} = m * A * h * d(\Delta T) \quad (8)$$

The trapped mass is known, and the cylinder geometry allows for the calculation of the wall area (A) available for heat transfer. The ΔT term is the difference between the cylinder contents temperature and the wall temperature. For this calculation method the wall temperature is assumed to be 550 K and treated as constant. The tests are run at steady-state conditions, so the assumption that the wall temperature is constant is justified. Finally, the heat transfer coefficient is an additional function of temperature. A well-established correlation developed by Hohenberg is utilized in this calculation method [19].

$$h = C_1 * V_c^{-0.06} * p^{0.8} * T^{-0.4} * (\bar{V}_p + C_2)^{0.8} \quad (9)$$

The cylinder volume is represented by V_c , p is the pressure, T is the mean gas temperature, and \bar{V}_p is the mean piston speed. The constants C_1 and C_2 which are 130 and 1.4 respectfully come from investigations done by Hohenberg. Part of that correlation includes the assumption that for diesel combustion, the radiation heat transfer is negligible.

The validity of these calculation methods have been demonstrated by [16, 20]. Additionally, more information on the supporting property calculations can be found in [17, 18]. Finally, an important parameter that is part of the heat release rate calculation is the mass fraction burned (MFB) profile. The heat release rate quantifies the fuel energy released at each increment during the calculation. If this parameter is integrated then the cumulative heat release is obtain as the total fuel energy released at any given point during the combustion process. If this parameter is then normalized by the total fuel energy delivered then the resulting value is the MFB. In other words the MFB profile

shows the percent of total fuel energy that has been consumed at any given time. These calculations are needed to analyze the engine completely. Without these terms, we would be limited to just measured parameters which would not give us much insight into the engine

2.5 Uncertainty Calculations

Uncertainty in a calculation is a non-negative parameter characterizing the dispersion of the values attributed to a measured quantity. The uncertainty has a probabilistic basis and reflects incomplete knowledge of the quantity. All measurements are subject to uncertainty and a measured value is only complete if it is accompanied by a statement of the associated uncertainty. The error bars in this study show the standard variations of the averaged data taken from the two days the conditions were run at. The variations between the two days presumably come from changes in ambient conditions like temperature, relative humidity, and barometric pressure.

3. RESULTS

For all cases, the fuel flow rate is constant, causing torque and BFCE to follow the same path, as shown in Figure 7. Both parameters reach a maximum then decrease as injection moves from its most retarded timing to its most advanced timing. When varying from -4° ATDC to -22° ATDC, the BFCE reaches a peak at -10° ATDC of 22.9%, while the minimum of 20.1% occurs at -22° ATDC. For higher load low speed cases, the maximum is reached at -13° ATDC and is 38.1%. For the high speed low load condition, the maximum of 20.4% is reached at -17.5° ATDC while the minimum of 18.8% is at -10° ATDC. For the high speed and high load test points, -22.5° ATDC produced the highest BFCE of 33.1% while -10° ATDC produced 30.2%. The average variation for all loads is 8.7% of the peak BFCE.

3.1 Effects of Injection Timing on Premixing

The first factor that directly affects the BFCE is the phasing of combustion which affects when and where energy is released in the combustion process. As it is known the longer the ignition delay the more premixing will occur during the combustion process. The longer ignition delay allows the fuel to interact with the air for longer periods of time. The long periods of time allow for atomization of the fuel so more fuel becomes premixed. In Figure 8, you will see the combustion ignition delay for the low speed

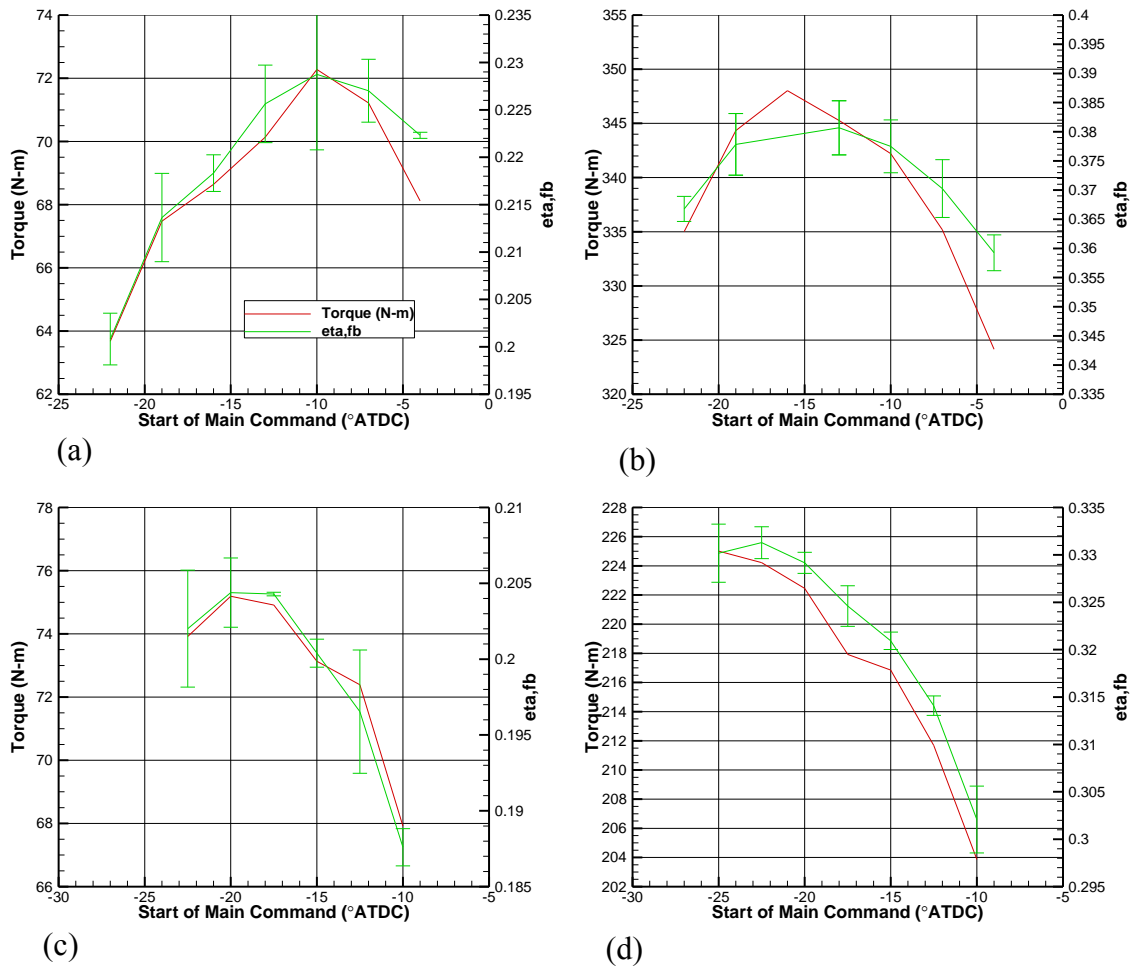


Figure 7: Torque and BFCE as Functions of Start of Main Command (in Degrees After Top Dead Center, or $^{\circ}$ ATDC) for (a) 1400 RPM/50 lb-ft, (b) 1400 RPM/250 lb-ft, (c), and 2400 RPM/50 lb-ft and (d) 2400 RPM/150 lb-ft.

cases studied in the research. The ignition delay follows a parabolic line. There is a minimum when start of main injection is around -10° ATDC as described by Heywood[8] for low to medium speeds. The longer the ignition delay the longer the fuel has to atomize and mix with the fuel so that larger fractions can combust in the premixed combustion phase.

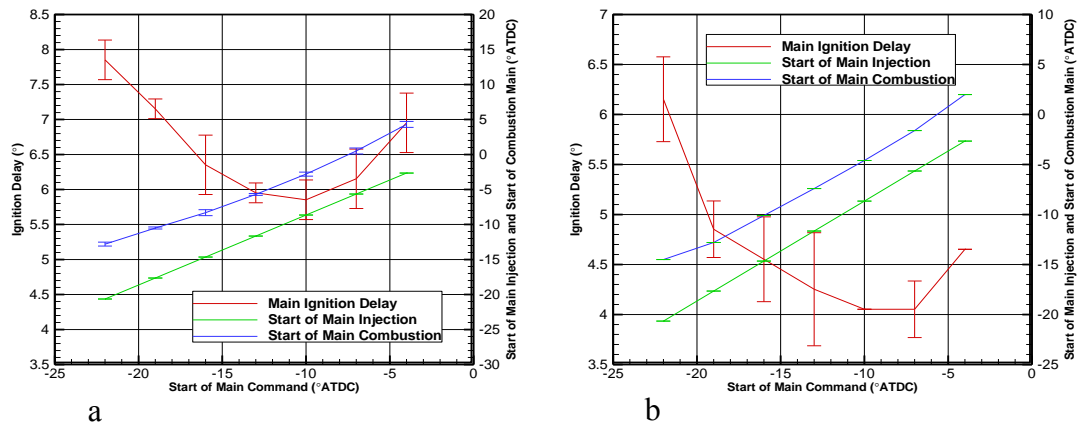


Figure 8: Ignition Delay, Start of Main Injection and Start of Main Combustion vs Start of Main Command for (a) 1400 RPM 50 lb-ft and (b) 250 lb-ft.

For the higher speeds, ignition delay does not follow such a clean pattern. In Figure 9, the sporadic nature of ignition delay can be seen for the 2400 RPM cases studied. There are also very high uncertainties related to each measurement so the analysis cannot be properly done. In the lower speed cases the factors controlling the ignition delay are air temperature and pressure changes that happen close to top dead center[2]. In the higher speeds there are other factors that must be taken into account for. The gas velocity inside the cylinder is much higher[9]. The actual time that the fuel is in contact with the air is less, but in general ignition delays are higher at higher speeds[4]. This is caused by the differences in the relationships between in cylinder conditions and time.

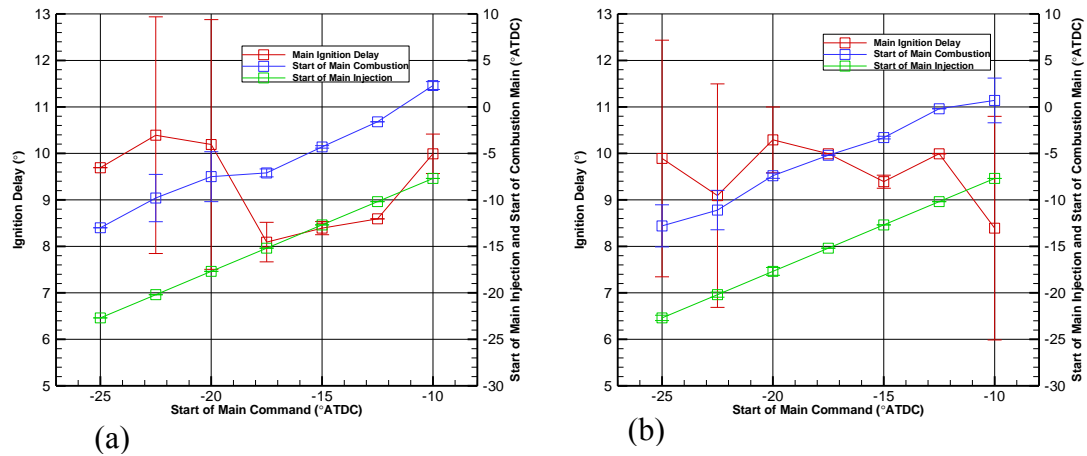


Figure 9: Ignition Delay, Start of Main Injection and Start of Main Combustion vs Start of Main Command for 2400 RPM (a)50 lb-ft and (b)150 lb-ft.

As the ignition delay increases the amount of premixed burning is increased. Larger portions of the fuel are burned during the premixed region. In Figure 10, this is illustrated by showing the mass fraction burned and rate of heat release for the 1400 RPM 50 lb-ft with injection timings for -10° ATD, and -22° ATDC because they have the shortest and longest ignition delay respectively. It can be seen that the slope of the mass fraction burned line for the -22° ATDC case is much steeper than the -10° ATDC case. Also, the size of the second hump in the heat release for the later injection is smaller than that of the earlier injection. This shows that more fuel in the -10° ATDC case is being burned in the 3rd phase of combustion instead of the more aggressive premixing phase. This is can also be seen in Figures 11-13 for the other cases examined in the study. Figure 11, shows the change in the amount of heat release in the mixing controlled combustion region better than the others. With the injection timing advanced, more fuel is burnt in the premixing for the -22° case so the rate of heat release for that

premixed combustion phase is higher than the mixing controlled section. But for the -10° case, there is not enough of an ignition delay to allow for much premixing so the majority of the heat release is done in the mixing controlled phase of combustion.

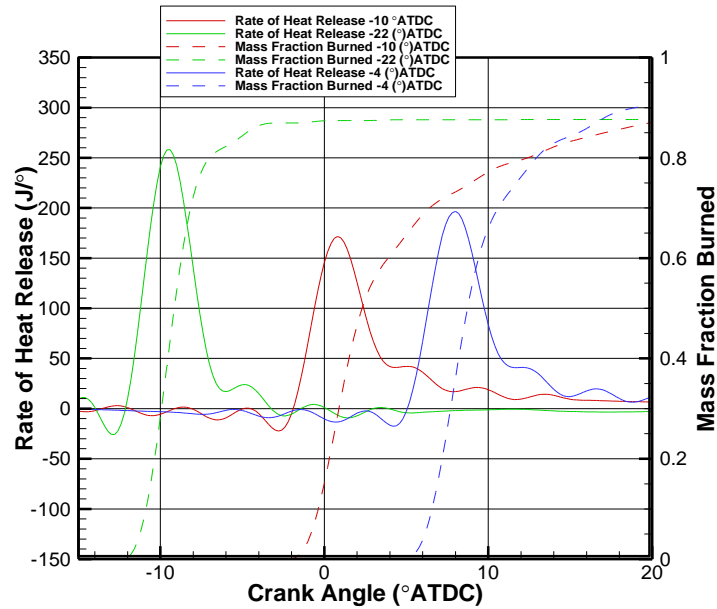


Figure 10: Rate of Heat Release and Mass Fraction Burned vs Crank Angle for 1400 RPM 50 lb-ft with Injection Timings of -4° , -10° , and -22° ATDC.

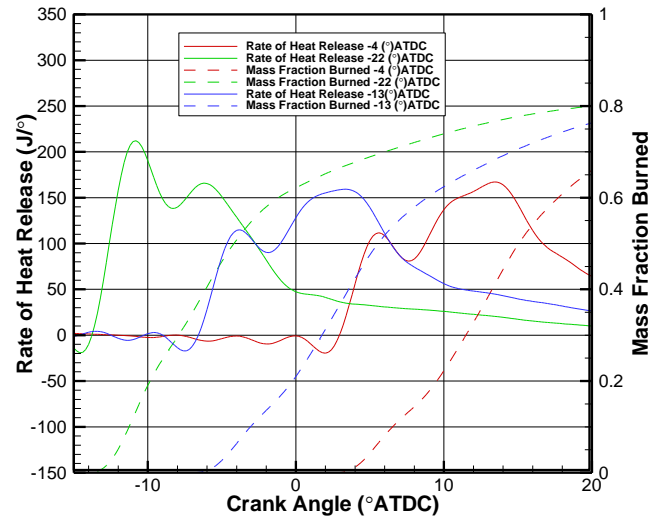


Figure 11: Rate of Heat Release and Mass Fraction Burned vs Crank Angle for 1400 RPM 250 lb-ft with Injection Timings of -4° , -13° , and -22° ATDC.

As seen before in the low load case the longer the ignition delay the more mass burned in the premixed region. For the -10° case, more fuel is actually burned in the mixing controlled phase then the premixed phase.

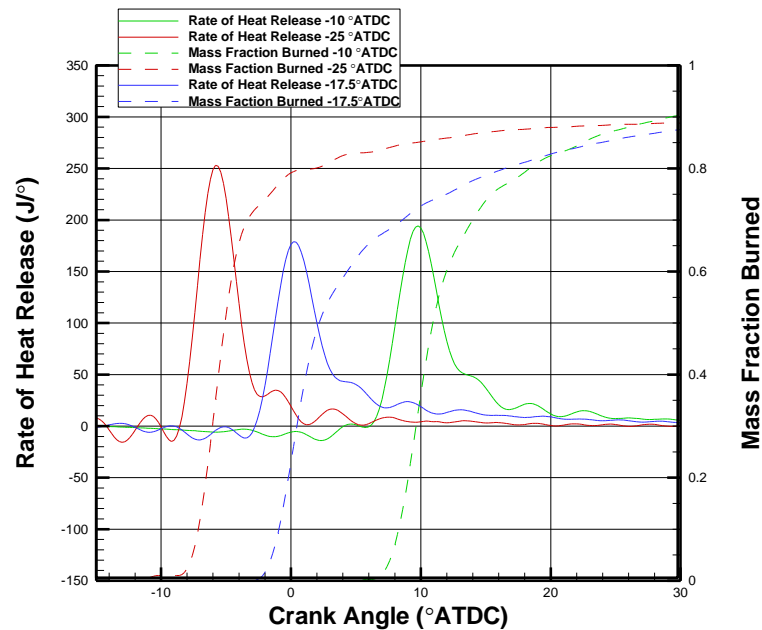


Figure 12: Rate of Heat Release and Mass Fraction Burned vs Crank Angle for 2400 RPM 50 lb-ft with Injection Timings of -10° , 17.5° , and -25° ATDC.

For the high speed low load case, the overall the pattern holds true as delay becomes longer heat release is quicker. Premixing effects BFCE because it leads to quicker combustion of larger portions of the fuel. If the ignition delay is timed right larger portions of the fuel will combust earlier in the engine leading to a more favorable combustion profile. A more favorable profile is one that balances negatives like heat transfer and compression loses with positives like high in cylinder pressure. The higher temperatures and pressure will lead to more heat transfer, compression loses, and effects other engine responses that will be discussed later at length.

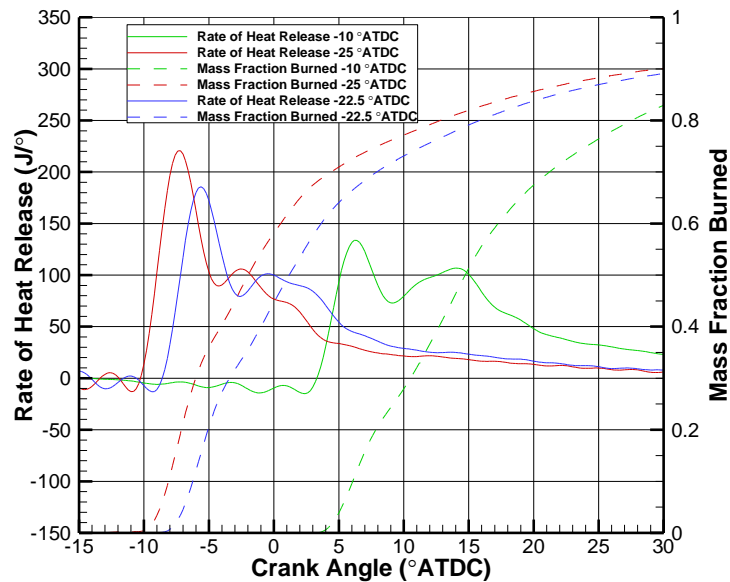


Figure 13: Rate of Heat Release and Mass Fraction Burned vs Crank Angle for 2400 RPM 150 lb-ft with Injection Timings of -10° , -22.5° , and -25° ATDC.

3.2 Effects of Injection Timing on Combustion Efficiency

As injection timing is moved further and further away from TDC the combustion efficiency raises to a maximum then falls off. The initial rise is due to more time for the fuel to vaporize and mix. It allows the fuel more time go through all the stages of combustion. The decrease comes from too much time. Fuel will penetrate too far into the cylinder and hit the walls also portions of the fuel may enter into zones where the equivalence ratio is not conducive to combustion. With the combustion efficiency increasing the energy available to do useful work also increases. With more energy being availed in the cylinder more energy can be lost to factors that make up the FMEP, PMEP, or ROHT. The changes in combustion efficiency, which can be seen in Figure

14, are very small though so the amount of energy that will be availed will not change radically.

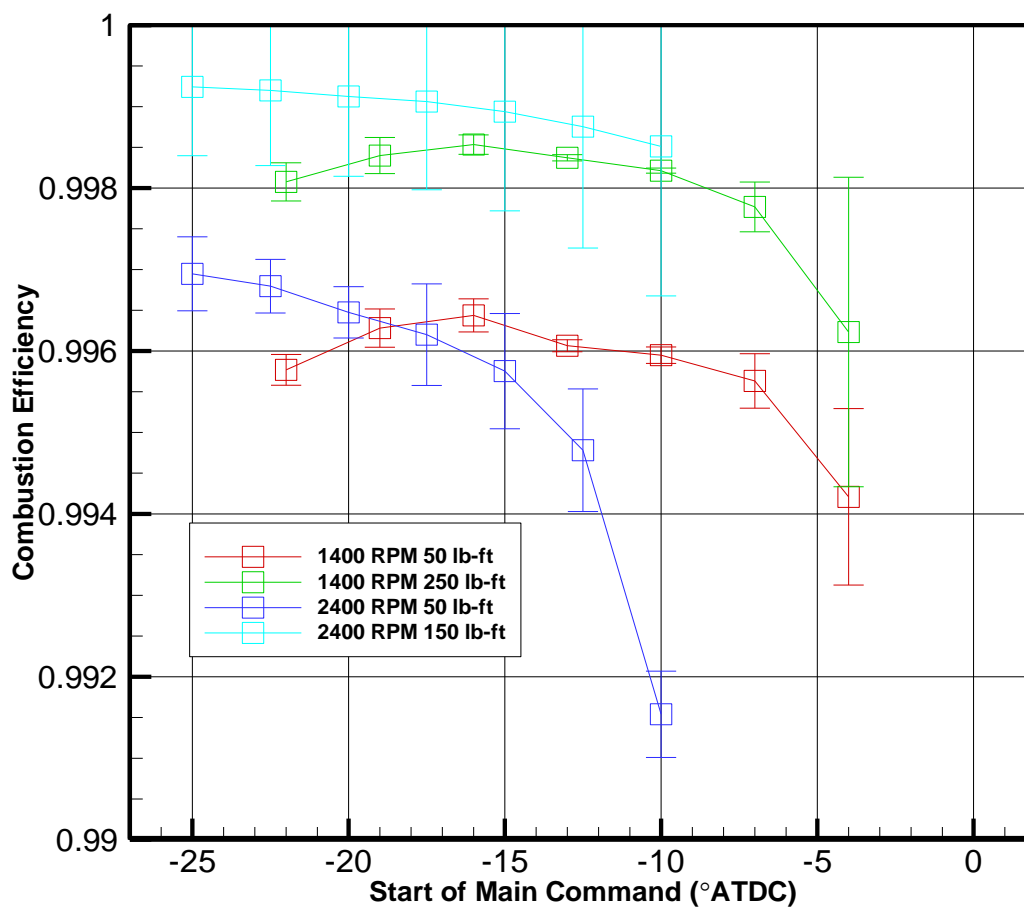


Figure 14: Combustion Efficiency vs Start of Main Command for All Speeds and Loads.

3.3 Effects of Injection Timing on In-cylinder Temperatures and Pressures

As injection timing is advanced higher in cylinder temperatures and pressures are reached. As injection timing is advanced the point at which ignition starts is also advanced. As the start of ignition is advanced, higher in cylinder pressures and

temperatures are reached. If the injections are advanced too much, the maximums will occur before TDC and cause compression losses. The temperature and pressure increase as the fuel combusts. Figure 15 shows the maximum temperatures and maximum pressures for both of the 1400 cases studied. The trend of increasing in-cylinder temperature and pressure with advancing of fuel injection holds. It is again confirmed by Figure 16 which shows the 2400 cases. The temperatures are calculated off the pressures. So discussion of the pressures is most applicable. As combustion is moved closer to TDC the pressure will rise because of the decreased volume available in the cylinder for the expanding gases.

Maximum temperature relate to BFCE, because with higher temperatures and higher pressures higher energy states are being reached. With a higher energy state being reached more energy is available to do useful work like create torque which would then increase the BFCE. The more torque available the more power is being created at the same speed which will in turn increase the BFCE because fuel flow rate is being held constant. So the portion of energy being converted from chemical energy being held in fuel to shaft work to the dynamometer will go up.

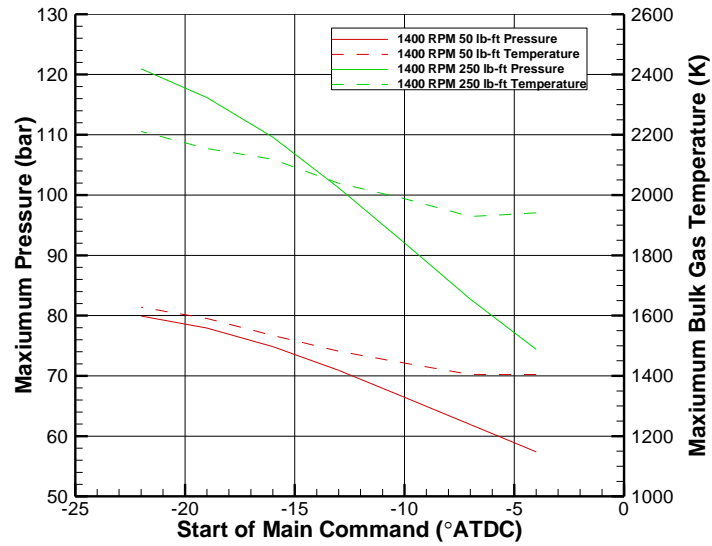


Figure 15: Pressure and Temperature Maximums vs Start of Main Command for the 1400 RPM Cases.

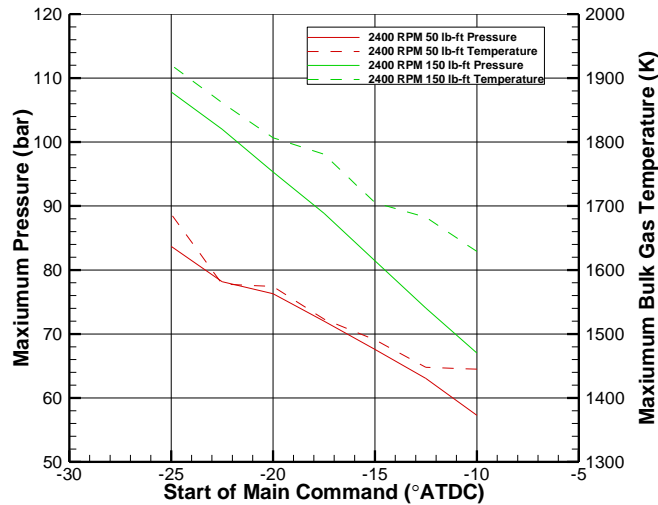


Figure 16: Pressure and Temperature Maximums vs Start of Main Command for the 2400 RPM Cases.

3.4 Effects of Injection Timing on Rate of Heat Transfer

As injection timing is advanced and in-cylinder temperatures and pressures go up so will heat transfer. Heat transfer is a function of cylinder volume, pressure, mean gas temperature, and mean piston speed. The total heat transfer equation is just the heat transfer coefficient multiplied by the surface area and the temperature difference between the mean wall temperature and the mean gas temperature. So as bulk gas temperature and in cylinder pressure rise heat transfer is forced to rise. In Figure 17, it can be seen as the injection timing at the low speed and low load conditions the heat transfer grows as the injection is being advanced. The same can be said for the low speed high load, high speed low load, and the high speed high and low cases which are illustrated in Figures 18-20.

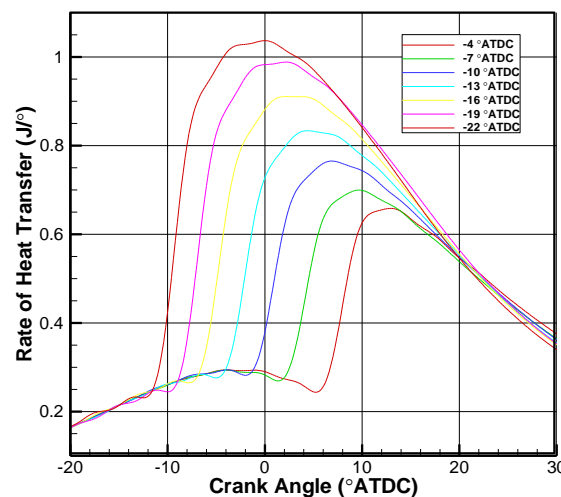


Figure 17: Rate of Heat Transfer vs Crank Angle for the 1400 RPM and 50 lb-ft Case.

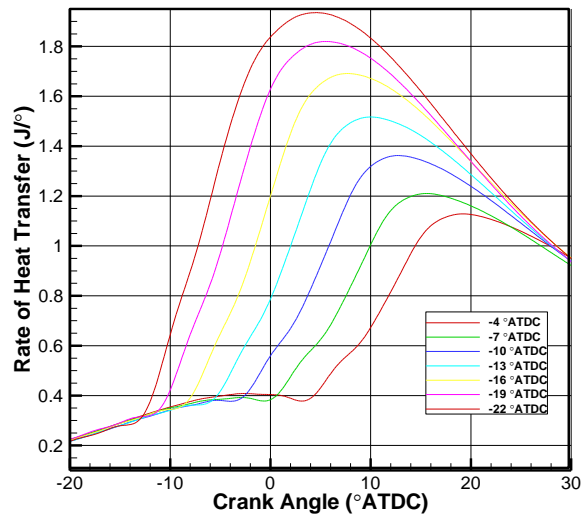


Figure 18: Rate of Heat Transfer vs Crank Angle for the 1400 RPM and 250 lb-ft Case.

As the injection timing is advanced the rate of heat transfer goes up that is due to the fact that the bulk gas temperature and in-cylinder pressure is going up as more and more fuel is burned earlier in the combustion cycle. With more fuel burning earlier in the combustion cycle, the expanding gases will start expanding in smaller volumes thus increasing the temperature and pressure. With more heat transfer out of the cylinder there will be less energy available to do useful work. The BFCE will begin to fall as more and more portions of the energy are lost to heat transfer. The heat transfer is one reason for the decrease in BFCE after the maximum is reached and injection timing is advanced further and further away from TDC.

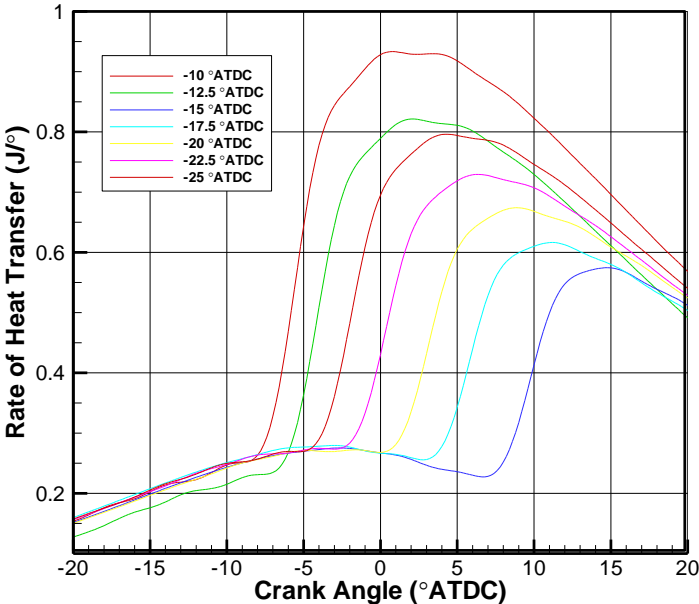


Figure 19: Rate of Heat Transfer vs Crank Angle for the 2400 RPM 50 lb-ft Case.

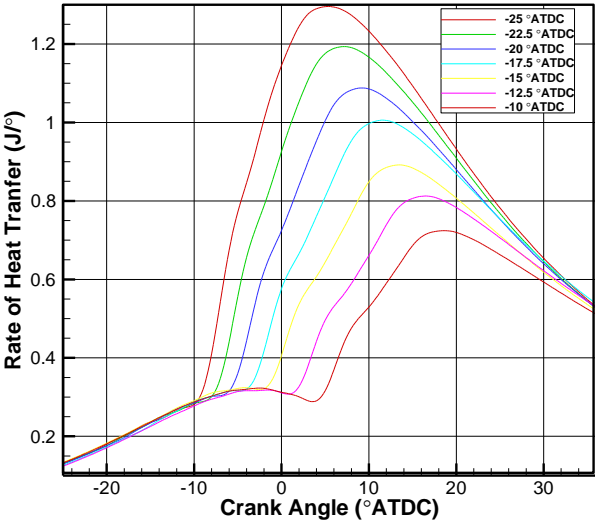


Figure 20: Rate of Heat Release vs Crank Angle for the 2400 RPM 150 lb-ft Case.

At the higher speeds everything is happening much quicker in time scale but the pattern still holds up. The ever increasing bulk gas temperature goes up thus causing more heat transfer out of the cylinder through the cylinder head, walls and piston.

The heat transfer coefficient will also affect how the rate of heat transfer acts. If you can recall Equation 8 from section 2.4.1, h is a function of pressure, temperature, piston speed, and volume. So as temperatures in the cylinder go up the heat transfer coefficient goes down but as the cylinder volume gets smaller the coefficient gets larger and the coefficient increases with pressure increases. The magnitude of the temperature component is much larger than the magnitude of the pressure and volume components. So on the compression stroke, the coefficient is going to get smaller as the temperature goes up even though the volume is getting smaller and the pressure is increasing. On the expansion stroke the coefficient is going to get larger because the temperatures are going to start decreasing. Just like in the compression stroke, because of the differences in magnitude the effects of volume and pressure are outweighed by temperature effects. As injection timing is advanced, h is going to decrease with the higher temperatures. Even though the coefficient is getting smaller the difference between the bulk gas temperature and the assumed wall temperature is getting bigger faster thus causing the apparent rate of heat release to go up. For the less advanced timings there are two peaks in the coefficient of heat transfer curves. The first peak is from the temperature effects on the coefficient of heat transfer but at the earlier injections the temperatures are not as high as in the more advanced timings consequently making the volume and pressure components more influential. These patterns can be seen in Figures 21 and 22, showing the low load

low speed case and the high speed high load case, respectively. The second bump in the high load high speed case is not as dramatic because the temperature change between the injection timings is not as vivid as in the low load low speed case.

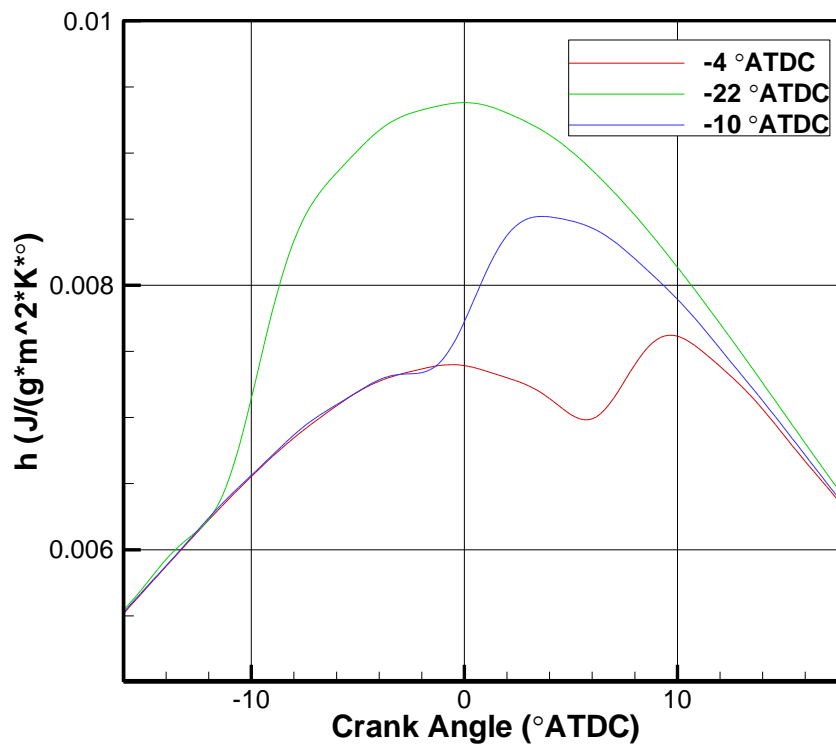


Figure 21: Heat Release Coefficient Vs Crank Angle in the Low Speed Low Load Case.

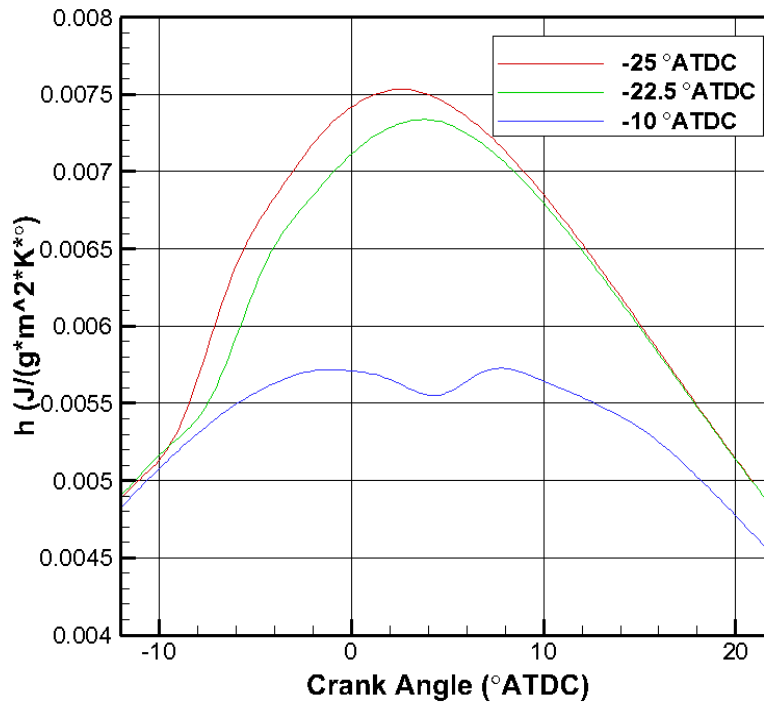


Figure 22: Heat Release Coefficient Vs Crank Angle in the High Speed High Load Case.

3.5 Effects of Injection Timing on Rate of Heat Transfer Due to Surface Area

Another aspect that will affect the heat transfer is the surface area available when the peak temperatures and pressures are reached. For injections with the peak pressure and temperature happening closer to TDC there will be less surface area in contact with the combustion gases decreasing the total heat transfer and the heat transfer coefficient. Take for instance the low speed low load case the maximum efficiency case is the -10° ATDC timing. The peak bulk gas temperature is after TDC and the majority of the temperature rise is just after TDC thus providing the most optimum conditions to minimize heat transfer through the walls of the cylinder. Figure 23 shows the bulk gas

temperature curve of the -10° ATDC as well as -4° ATDC and -22° ATDC timings. For the -4° ATDC case it has lower temperatures but the temperatures do not begin to rise until 6° ATDC. The late temperature increase will cause expansion losses and because there is a larger portion of the heat release happening with more surface area a larger portion of the available energy will be transferred through the walls. With the more expansion losses and heat transfer, the fuel will not be as efficiently transformed into mechanical work in the form of torque thus causing BFCE to decrease. For the -22° ATDC timing, the temperatures are much higher than the other cases, but because they happen so much further before TDC there are a lot of compression losses incurred plus higher temperatures are in contact with more surface area for longer periods of time. The BFCE will then again decrease because the available energy will not be as efficiently transformed into torque being delivered to the dynamometer.

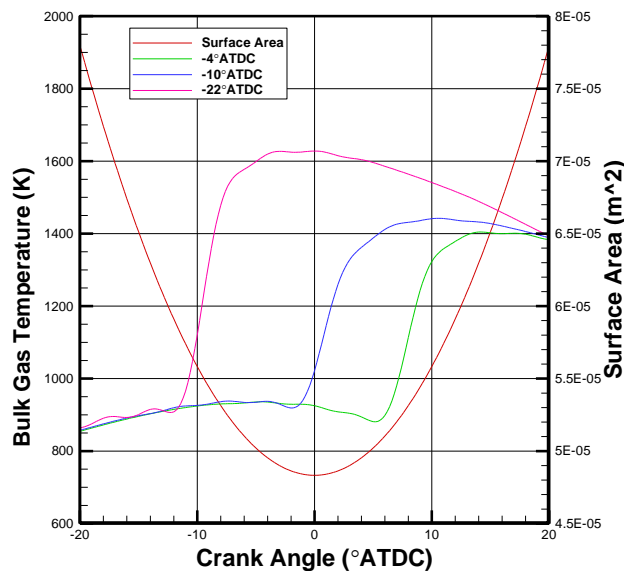


Figure 23: Bulk Gas Temperature (K) and Surface Area (m²) vs Crank Angle (°) for the -4°, -10°, and -22° ATDC Timings of the Low Speed Low Load Test Conditions.

The pattern holds true throughout the rest of the conditions, as can be seen in Figures 24-26.

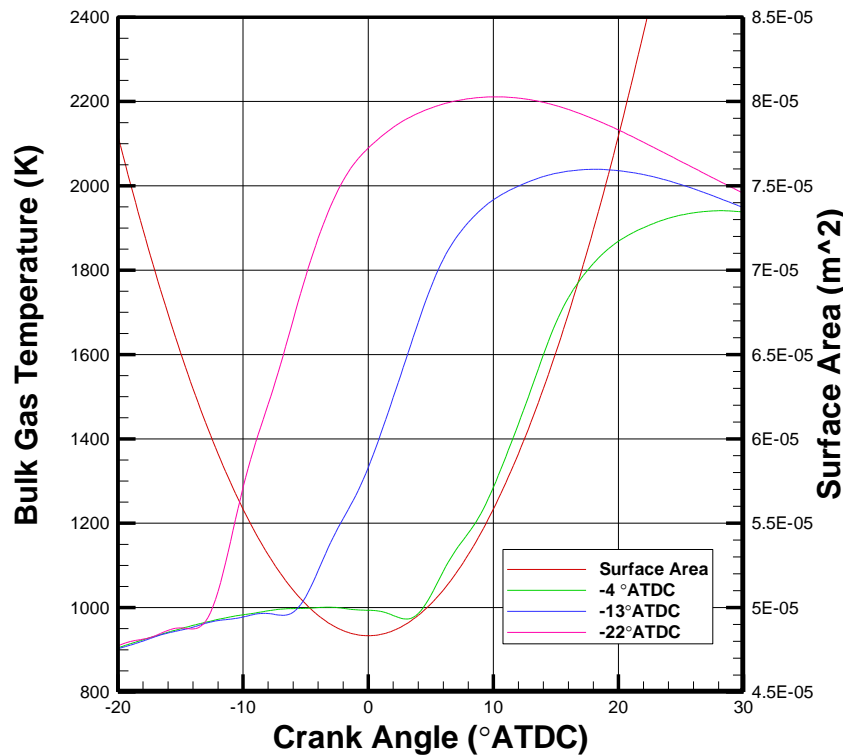


Figure 24: Bulk Gas Temperature (K) and Surface Area (m²) vs Crank Angle (°) for the -4°, -13°, -22° ATDC Injection Timings for the Low Speed High Load Case.

Again the timing with the highest efficiency, -13° ATDC, has the most optimum temperature to surface area alignment. The earlier injection has lower temperatures but the majority of the expansion is happening later in the expansion stroke as a consequence increasing the expansion losses. The most advanced injection, -22° ATDC, has much higher temperatures which leads to higher heat transfer but also the temperatures are happening before TDC which will cause compression losses in the engine as a result decreasing the BFCE.

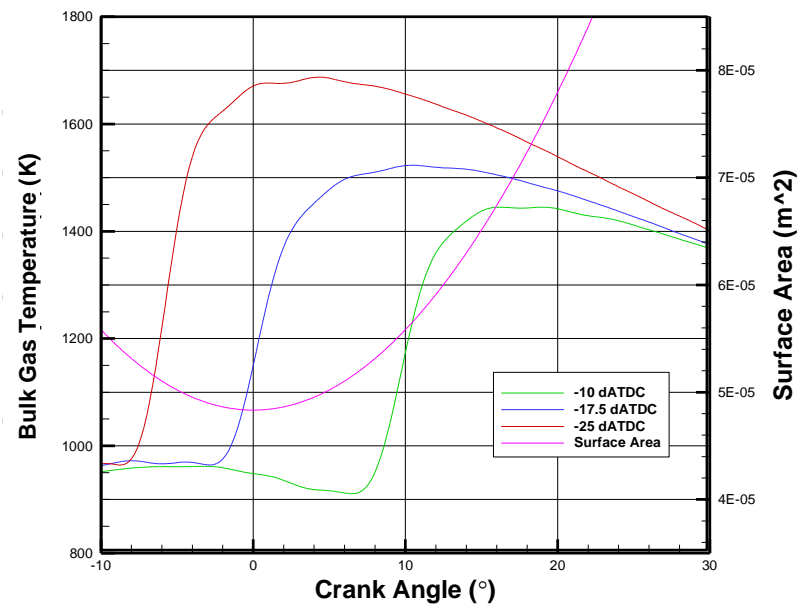


Figure 25: Bulk Gas Temperature (K) and Surface Area (m^2) vs Crank Angle ($^\circ$) for the -10° , -17.5° , -25° ATDC Injection Timings for the High Speed Low Load Case.

For the high speed low load case the pattern continues. With the earliest injection timing, -10° ATDC, the much lower bulk gas temperature at the start of the temperature rise is due to the fact that combustion is happening so much further past TDC that temperatures start to decrease due to expansion.

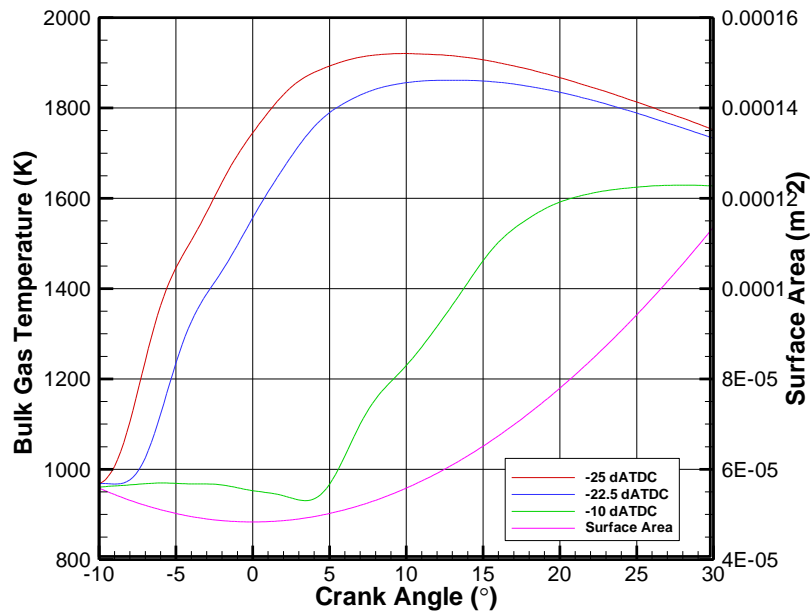


Figure 26: Bulk Gas Temperature (K) and Surface Area (m²) vs Crank Angle (°) for the -10°, -22.5°, -25° ATDC Injection Timings for the High Speed High Load Case.

For the high speed high load case, the temperature profiles do not as closely follow the pattern but that is just because the peak efficiency injection timing, -22.5° ATDC, is so close to the most advanced - 25° ATDC injection timing. Put the pattern still holds true. The most advanced injection timing has higher bulk gas temperatures before TDC which will cause more heat transfer and higher pressures before TDC which will increase compression losses those reducing the power out of the engine and decreasing the BFCE. With the temperature rise happening after TDC the earliest injection timing -10° ATDC experiences expansion losses those decreasing the power out of the engine and decreasing the BFCE.

3.6 Effects of Injection Timing on Mean Effective Pressures

IMEP increases at the beginning until MBT which is because of the increasing in-cylinder pressure and the combustion phasing being more favorable. It then decreases more rapidly as combustion is phased to where peak pressures are occurring before TDC. The peak pressures cause the indicated work to go down which will also cause the brake work to go down. As seen in Equation 2, FMEP, BMEP, and IMEP are directly correlated with one another. So as IMEP and FMEP decrease BMEP will decrease as well. BMEP does not decrease as quickly as IMEP because FMEP decreases more leisurely throughout the injection timing sweep. So BMEP and IMEP increase up to the most efficient injection timing with respect to BFCE then begins to decrease after the maximum is reached. This is evident in Figures 27 and 28 which represent the low load low speed case and the high speed high load case respectively.

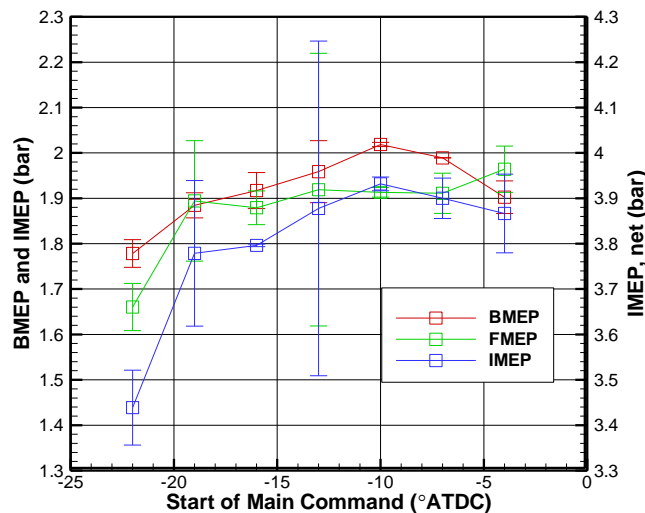


Figure 27: Net Indicated Mean Effective Pressure, Brake Mean Effective Pressure, and Friction Mean Effective Pressure vs Start of Main Command for Low Speed and Low Load Case.

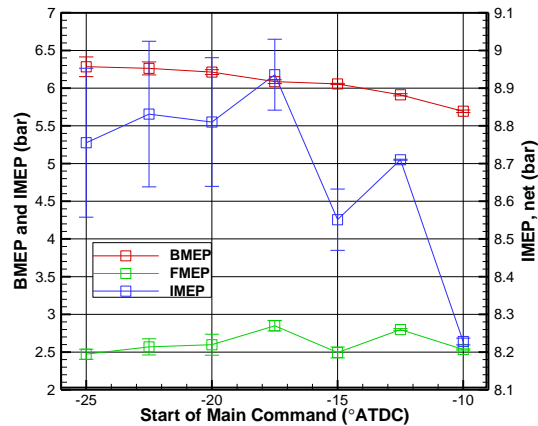


Figure 28: Net Indicated Mean Effective Pressure, Brake Mean Effective Pressure, and Friction Mean Effective Pressure vs Start of Main Command for the High Speed High Load Case.

3.7 Effects of Injection Timing on Intake and Exhaust Manifold Pressures and Turbocharger Speed

As injection timing is advanced the exhaust manifold pressure tends to decrease. As the exhaust manifold pressure decreases with the VGT set at a constant vane position the turbo speed will go down. This will cause the intake manifold pressure to decrease as well. This is all due to the available energy left in the exhaust gases. With combustion phased later in the expansion stroke gases are going to be much hotter when they expelled from the cylinder during the exhaust stroke of the engine. This will make them at a higher energy state than at advanced injection timings. The higher energy states deliver more energy to the turbo thus causing it to spin faster and compress more air to be inducted into the cylinder. Because the EGR valve is closed, all the exhaust gases must flow through the turbocharger. At a constant engine speed there are many variables that can affect the intake manifold pressure, but they have been insulated as best they

could be to show a dependence on injection timing. Figures 29 and 31-33 show the intake and exhaust manifold pressures and the turbo speed versus the start of main command for all the speeds and loads tested.

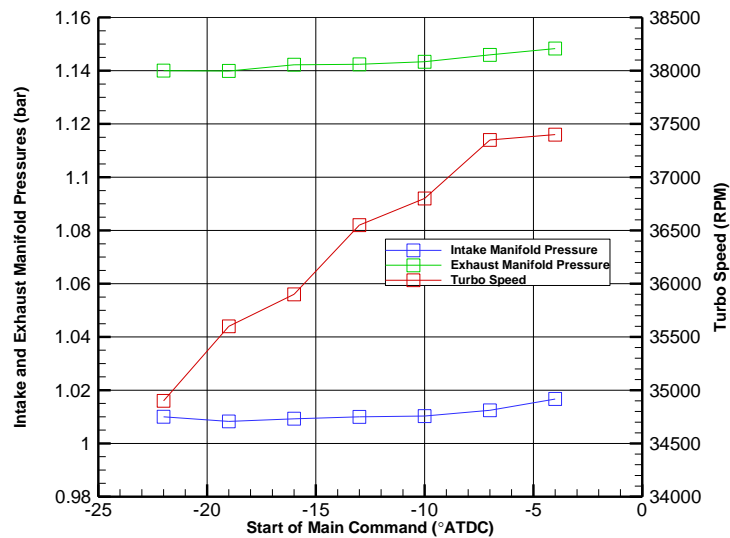


Figure 29: Intake and Exhaust Manifold Pressures and Turbo Speed vs. Start of Main Command for Low Speed Low Load Test Condition.

For the low speed and low load case the pressure changes are very minimal, because there is so little boosting going on. This was because the turbo vane position was held constant during the entirety of the test matrix so it was not optimized for the low speed load test condition, however the pattern holds true. The exhaust manifold pressure drops as timing is advanced, which causes a smaller pressure gradient between the exhaust manifold and the exhaust pipe causing the turbocharger to slow down and decrease the amount of air entering the intake manifold which causes the intake manifold pressure to decrease as well. The exhaust manifold temperatures do not change as much as in other test conditions. Figure 30 shows the exhaust manifold temperature versus

Start of Main Command for the entire test matrix. The decrease in temperature for the low load case is not as steep as the decrease for the high load case at the same speed

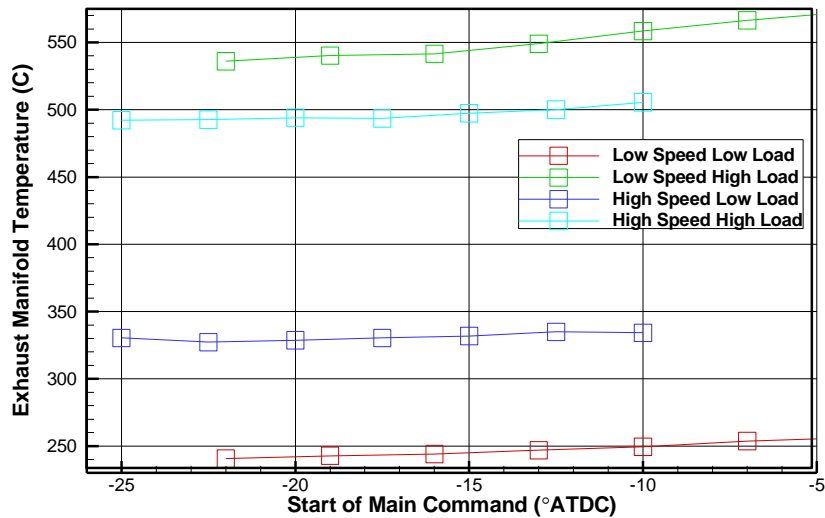


Figure 30: Exhaust Manifold Temperature vs. Start of Main Command for All Test Conditions.

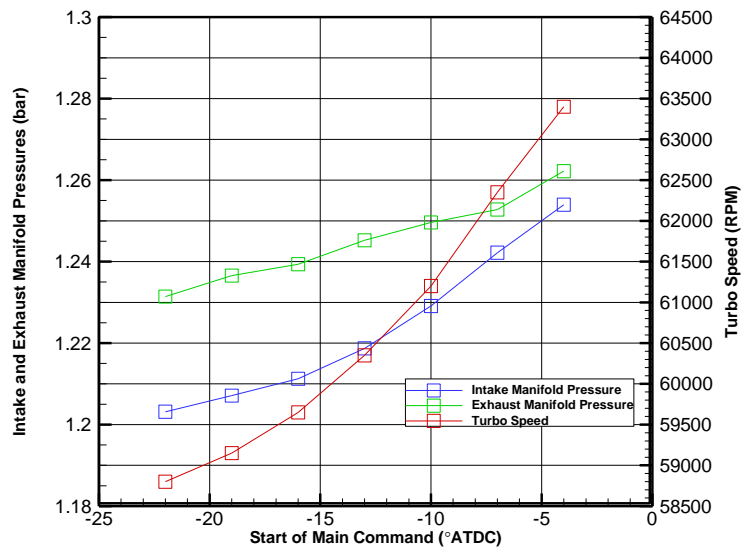


Figure 31: Intake and Exhaust Manifold Pressures and Turbo Speed vs. Start of Main Command for Low Speed High Load Test Condition.

Unlike for the low speed low load test conditions, the low speed high load condition has a much more noticeable pressure drop as the injection timings are advanced. The exhaust gas temperatures from the earlier injections are higher than the more advanced ones which causes a higher pressure gradient between the exhaust manifold and the exhaust pipe through the turbo charger. These higher pressure differences allow the turbocharger to do more work from the unclaimed energy in the exhaust gases. It would lend one to believe that if the turbocharger is reclaiming more unused energy the engine is going to become more efficient however that is not the fact. Because the engine is expelling higher energy states of the exhaust gas that means the energy was not used in the most useful manner. The energy that is able to be converted into actual torque is much more important to the overall efficiency of the engine than the energy used to induct more air into the engine.

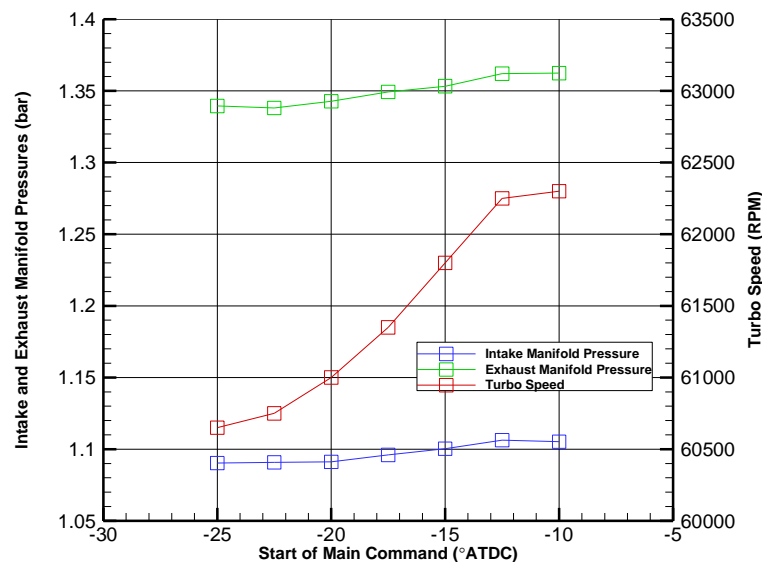


Figure 32: Intake and Exhaust Manifold Pressures and Turbo Speed vs. Start of Main Command for High Speed Low Load Test Condition.

The pattern holds for the high speed low load condition as well. And just like the other low load case the decreases in intake and exhaust pressure are not as steep. This is because there is not as much of a temperature difference between the earlier and later injection timings at the high speed low load test condition.

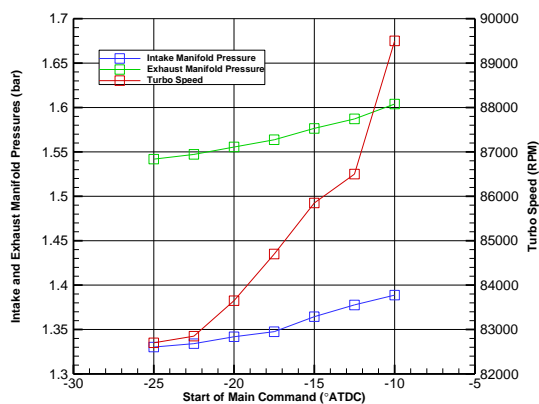


Figure 33: Intake and Exhaust Manifold Pressures and Turbo Speed vs. Start of Main Command for High Speed High Load Test Condition.

The high speed high load case keeps to decreasing patterns as well. Just like in the low speed tests the differences are much greater in the high load conditions than the low load. This is again because of the exhaust gas energy difference between the states that is evident in the differences in the exhaust manifold temperatures. The earlier the injection timing is the more energy that will be lost in the exhaust gases. The turbo charger tries to counteract this by reclaiming some of the wasted energy, but the energy

it reclaims is not as valuable to the engine as if the energy was used in the expansion stroke. The amount of energy that is reclaimed in the turbo charger does not equate to the same amount of energy being gained by the engine by inducting more air at a higher pressure.

3.8 Effects on Location of Peak Pressure

Fuel injection timing will affect the location of peak pressure by changing the timing and phasing of combustion. As injection timing is advanced, the location of peak pressure moves closer and closer to TDC as seen in Figure 34. In this study, the location of peak pressure never reaches TDC, but it does come close. There is a pattern though when BFCE is plotted verses location of peak pressure. The BFCE increases until location of peak pressure is between 5° and 6° ATDC. This is true for all cases and loads. In the low load cases, illustrated by Figure 35, the peak efficiencies happen around location of peak pressure equal to 5° ATDC. For the high load cases, illustrated by Figure 36 for the low speed case the peak efficiency corresponds to a peak pressure location of 6° degrees and for the high speed case the location of peak pressure that brings the highest efficiency is 5° ATDC. The 5° to 6° ATDC “sweet spot” is because these are the injection timings that balance out expansion loses and compression loses with things like heat transfer out of the cylinder. With injection timings that allow for the location of peak pressure to fall in the “sweet spot”, the efficiency will be higher than those who do not, because they will either have too much energy lost to compressing the

expanding hot gases that occur in the most advanced timings or too much energy not being used in the cylinder to do useful work like the least advanced timings.

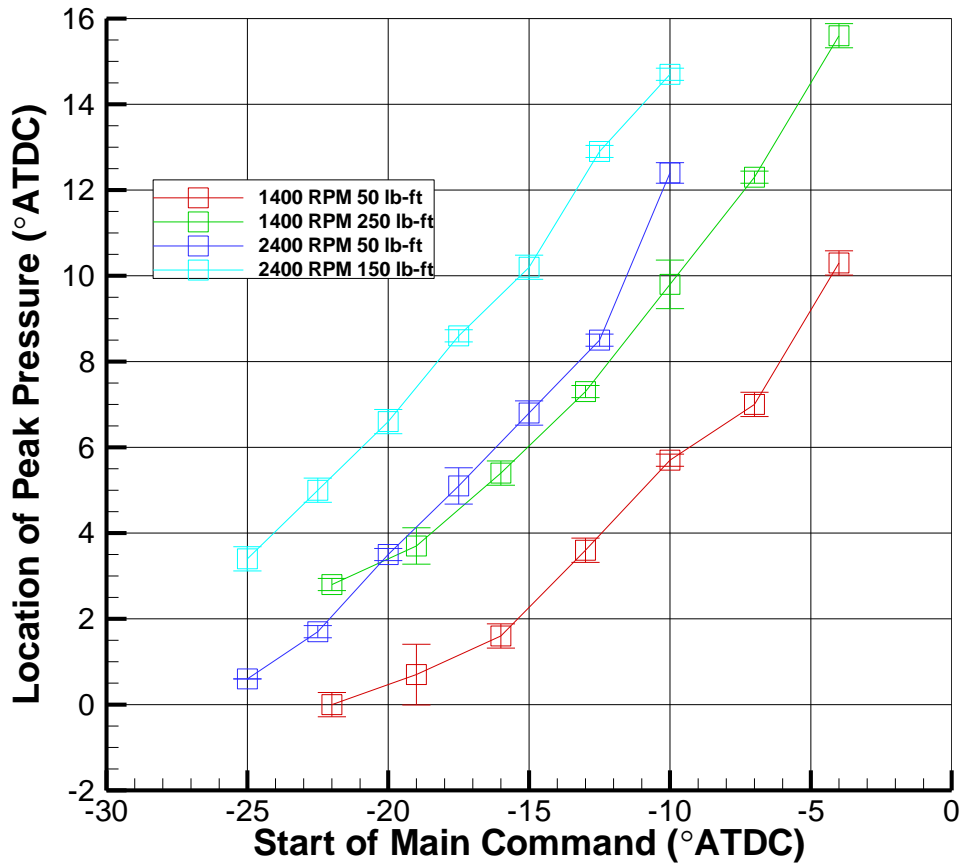


Figure 34: Location of Peak Pressure versus Start of Main Command for All Test Conditions.

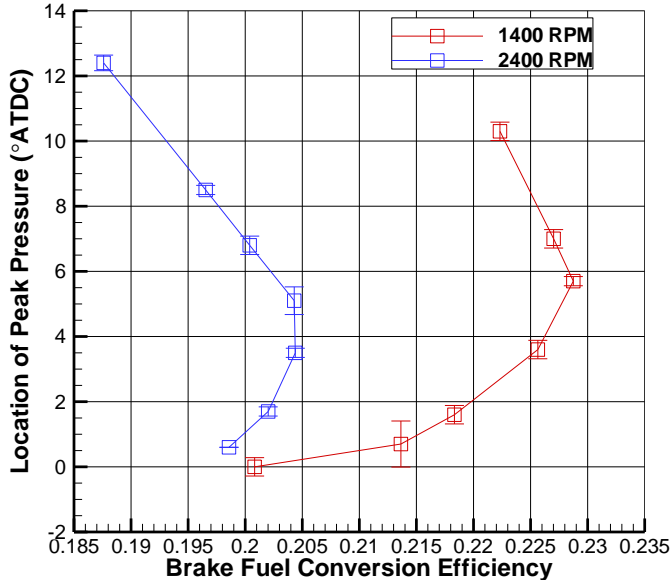


Figure 35: Location of Peak Pressure versus Brake Fuel Conversion Efficiency for Low Load Cases.

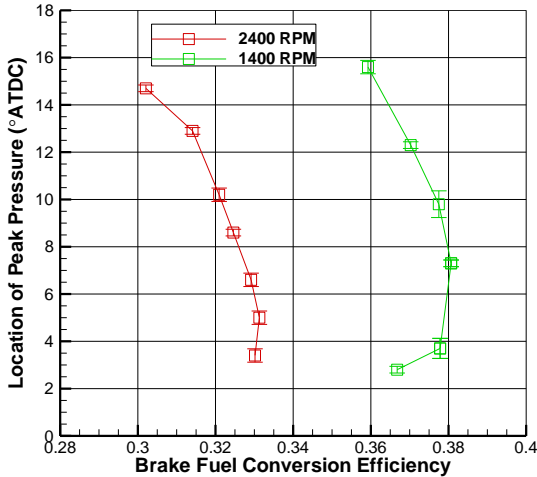


Figure 36: Location of Peak Pressure versus Brake Fuel Conversion Efficiency for High Load Cases.

4. CONCLUSIONS AND SUMMARY

This research study was able to characterize how the engines brake fuel conversion efficiency was affected by variations in injection timing. It was also able to characterize how the combustion process which is influential to the brake fuel conversion efficiency responded to injection timing changes. This testing will allow for more research in the future into the fundamentals of the combustion process and how changing a single parameter can affect the entire engine. The following conclusions can be made from the study.

- As fuel injection is advanced, BFCE will reach a maximum then decrease back down.
- The increase in BFCE up to the maximum results from decreasing mixture temperatures – consequently decreasing rates of heat transfer – as combustion shifts to later in the cycle.
- The decrease in BFCE after its peak results from decreased expansion of the thermal energy, as combustion shifts to too late in the cycle.
- As the injection timing is advanced the exhaust gas temperatures decrease thus causing the exhaust manifold pressure to decrease which lowers the pressure gradient through the turbocharger and decreases the intake manifold pressure. As injection timing is advanced the maximum bulk gas temperature and the in-cylinder pressure rise, because of the decreasing volumes that the reacting gases come into contact with.

- The combustion profile becomes more favorable for peak BFCE as injection is advanced up to a point then begins to degrade again. The cause of the more favorable combustion profiles is because of the quicker burn rates associated with more premixed combustion. The cause of the decline in the combustion profile is because of too early of a start of combustion with the most advanced injection timings. With injection timing being advanced, longer combustion delays allow for more of the fuel to be burnt during the premixed combustion phase.
- Turbocharger speeds decrease as injection timing is advanced, because the exhaust manifold pressures are decreasing making the pressure gradient across the turbocharger smaller. With a smaller pressure gradient, there is less available energy to drive the turbocharger with its fixed vane position.
- Injection timings with the location of peak pressure occurring around 5° to 6° ATDC allow for the peak brake fuel conversion efficiencies because the favorable heat release and pressure profiles that mitigate losses so the most amount of energy is used to do useful work during the power stroke of the engine.

REFERENCES

- [1] Lyn, W. T., and Valdmanis, E., 1968, "Effects of physical factors on ignition delay," *Automotive Engineering Congress and Exposition*, SAE International, Detroit, Michigan.
- [2] Plee, S. L., and Ahmad, T., 1983, "Relative roles of premixed and diffusion burning in diesel combustion," *SAE International Fall Fuels and Lubricants Meeting and Exhibition*, SAE International, San Francisco, California.
- [3] Kamimoto, T., and Kobayashi, H., 1991, "Combustion processes in diesel engines," *Progress in Energy and Combustion Science*, **17**(2), pp. 163-189.
- [4] Kouremenos, D. A., Hountalas, D. T., Binder, K. B., Raab, A., and Schnabel, M. H., 2001, "Using advanced injection timing and EGR to improve DI diesel engine efficiency at acceptable NO and soot levels," *SAE 2001 World Congress*, SAE International, Detroit, Michigan.
- [5] Kook, S., Bae, C., Miles, P., Choi, D., and Pickett, L., 2005, "The influence of charge dilution and injection timing on low-temperature diesel combustion and emissions." SAE Paper 2005-01-3837, 2005
- [6] Stringer, V., Cheng, W. L., Lee, C. F. F., and Hansen, A., 2008, "Combustion and emissions of biodiesel and diesel fuels in direct injection compression ignition engines using multiple injection strategies," SAE Technical Paper 2008-01-1388
- [7] Wakuri, Y., Soejima, M., Ejima, Y., Hamatake, T., and Kitahara, T., 1996, "Studies on friction characteristics of reciprocating engines," *SAE Transactions*, **104**, pp. 1463-1477.
- [8] Heywood, J. B., 1988, *Internal Combustion Engine Fundamentals*, McGraw-Hill, Inc., New York, New York.
- [9] Austen, A., and Lyn, W., 1960, "Relation between fuel injection and heat release in a direct injection engine and the nature of the combustion processes," *ARCHIVE: Proceedings of the Institution of Mechanical Engineers, Automobile Division 1947-1970, 1960*, pp. 47-62.
- [10] Hountalas, D., "The effect of operating parameters on the net and gross heat release rates of a direct injection diesel engine," *In: Proceeding of the Second Biennial ASME-ESDA International Conference on Design of Energy Systemes*, **63** (3), 1994.

- [11] Lyn, W. T., 1962, "Study of burning rate and nature of combustion in diesel engines," Symposium (International) on Combustion, **9**(1), pp. 1069 - 1082.
- [12] Lee, J., 2011, "Experimental investigation of thermal load in high speed direct injection diesel engine under the control of various engine performance parameters," Journal of Engineering for Gas Turbines and Power, **133**, p. 032802.
- [13] Media, V., 2003, "The New Diesel Powered Volvo XC70 D5," http://www.motorsportscenter.com/article_165.shtml.
- [14] Systems, J. D. P., 2006, *2006 Service Manual*, John Deere, Waterloo, IA.
- [15] Randolph, A. L., 1990, "Cylinder-pressure-transducer mounting techniques to maximize data accuracy," *SAE International Congress and Exposition, SAE International*, Detroit, Michigan, SAE Paper 900170, 1990.
- [16] Depcik, C., Jacobs, T., Hagen, J., and Assanis, D., 2007, "Instructional use of a single-zone, premixed charge, spark-ignition engine heat release simulation," International Journal of Mechanical Engineering Education, **35**(1), pp. 1-31.
- [17] Krieger, R. B., and Borman, G. L., 1966, "Computation of apparent heat release for internal combustion engines," ASME Paper No. 66-WA/DGP-64.
- [18] Brunt, M. F. J., and Platts, K. C., 1999, "Calculation of heat release in direct injection diesel engines," SAE Transactions - Journal of Engines, **108**(SAE Paper No. 1999-01-0187), pp. 161-175.
- [19] Hohenberg, G. F., 1979, "Advanced approaches for heat transfer calculations," SAE Transactions, **88**(SAE Paper No. 790825), pp. 2788-2806.
- [20] Foster, D. E., 1985, "An overview of zero-dimensional thermodynamic models for IC engine data analysis," *SAE International Fall Fuels and Lubricants Meeting and Exhibition, SAE International*, Tulsa, Oklahoma, SAE Paper No. 852070.
- [21] Chase, M. W., 1998, *NIST-JANAF Thermochemical Tables*, American Chemical Society, Washington, D.C.

VITA

Name: James Elliott McLean Jr.

Address: 3123 TAMU
College Station, TX 77840

Email Address: james.mclean.jr@gmail.com

Education: B.S., Mechanical Engineering, The University of Alabama, 2009
M.S, Mechanical Engineering, Texas A&M University, 2011